Journal of Geosciences, 59 (2014), 41–68 DOI: 10.3190/jgeosci.156

Original paper

Late Variscan calc-alkaline lamprophyres in the Krupka ore district, Eastern Krušné hory/Erzgebirge: their relationship to Sn–W mineralization

Miroslav ŠTEMPROK*, David DOLEJŠ, František V. HOLUB

Institute of Petrology and Structural Geology, Charles University, Albertov 6, 128 43 Prague, Czech Republic; miroslav.stemprok@natur.cuni.cz
* *Corresponding author*

Variscan lamprophyres occur in the greisen tin-, tungsten- and molybdenum-ore district of Krupka in the Eastern Krušné hory/Erzgebirge (KHE). They belong to a bimodal dyke suite of aplites, felsic porphyries, microgranites and mafic dykes associated with late Variscan tin-bearing granites and include minettes, kersantites and spessartites, while vogesite reported earlier has not been confirmed. One altered mafic dyke is interpreted as original microdiorite. All lamprophyres are basic to intermediate rocks (47.3–56.9 wt. % SiO_2) with shoshonitic to ultrapotassic composition (3.1–7.5 wt. % K_2O). The high concentrations of MgO (4.7–11.4 wt. %), molar Mg/(Mg + Fe) ratios (0.56–0.74) and abundances of compatible elements (350–800 ppm Cr, 130–360 ppm Ni) indicate that lamprophyres represent primary mantle melts that underwent no or little fractionation or contamination, and high LREE/HREE ratios point to magma formation in the stability field of garnet peridotite. In addition, high contents of potassium and LILE (50–370 ppm Li, 150–920 ppm Rb, 750–3100 ppm Ba) indicate metasomatic enrichment of the upper mantle prior to partial melting. The LILE–HFSE–REE patterns indicate involvement of slab components (subducted siliciclastic and carbonate sediments). Strong enrichment in U (6–29 ppm) and Th (17–75 ppm) is another characteristic feature of lamprophyres from the Eastern KHE and elsewhere in central Europe, and it is consistent with the metasomatic transport *via* oxidized saline fluids from the slab to the mantle wedge. The lamprophyres in the Krupka district were variably greisenized in the vicinity of granite greisens and Sn–W hydrothermal veins and their original minerals were replaced by an assemblage of lithian phlogopite, topaz, fluorite, apatite and titanium-bearing phases. During alteration, they were strongly depleted in Na_2O, CaO, Sr and Ba, moderately depleted in REE, and enriched in Li, Rb, Cs, Sn and F. By contrast, Al and Zr behaved as immobile elements and their abundances indicate overall mass loss of 10–18 % during greisenization consistent with the increase of porosity, which facilitated the hydrothermal dissolution–precipitation reactions. The spatial association of greisens and lamprophyres suggests that the greisenizing fluids migrated along similar geological structures, which were previously accessible to the mantle-derived media (melts and/or fluids). On a local scale, the lamprophyre dykes intersected by greisen veins provided geochemical or lithological barrier, which favoured the cassiterite deposition. The timing of lamprophyre dykes also indicates that the mantle metasomatism beneath the KHE area occurred before the late Variscan granitic magmas were generated.

Keywords: lamprophyres, greisenization, Li mica composition, mantle metasomatism, Krušné hory/Erzgebirge, Bohemian Massif
Received: 29 July 2013; accepted: 26 November 2013; handling editor: V. Rapprich

1. Introduction

Lamprophyres are a specific group of mafic dyke rocks with mafic hydrous silicates – dark micas and amphiboles – forming phenocrysts while feldspars are confined to the groundmass (Woolley et al. 1996). They are considered to be the product of melting of metasomatized mantle above ancient subduction zones as demonstrated by their high contents of compatible major and trace elements (e.g., MgO, Cr, Ni, mg#) as well as incompatible trace elements (e.g., Cs, Rb and Li). Their high volatile content has often been considered as important in ore-forming processes caused or contributed by magmatic fluids (Rock 1991). The association of calc-alkaline lamprophyres with silicic batholiths poses a long-standing problem regarding the genetic relationship between the sources of mafic and felsic magmas. Post-collisional magmatism includes voluminous granitic rocks that were mostly derived by crustal melting (e.g., Sylvester 1998; Bonin 1990). By contrast, subduction of altered oceanic crust, oceanic sediments or continental crust results in metasomatism of the mantle wedge (Guo et al. 2004; Janoušek and Holub 2007; Abdelfadil et al. 2013) where late-orogenic lamprophyre magmas, in particular calc-alkaline lamprophyre types, form (Turpin et al. 1988; Awdankiewicz 2007; Seifert 2008). These varieties are common in magmatic and metamorphic units of the Bohemian Massif, especially along the terrane boundaries

of the Moldanubian, Saxothuringian and Lusatian zones (e.g., von Seckendorff et al. 2004; Awdankiewicz 2007; Krmíček 2010). Some of these dyke rocks correspond to lamproites (Holub 2003; Krmíček et al. 2011) and might thus be close to the lamprophyre primary magmas observed in the Mediterranean area of southern Europe (Prelević et al. 2004).

Lamprophyres have been repeatedly considered as important for the origin of gold mineralization (McNeil and Kerrich 1986; Wyman and Kerrich 1988; Rock et al. 1989; Ashley et al. 1994; Lobach-Zhuchenko 2000) and also for diverse mineralization styles in the Variscan Krušné hory/Erzgebirge (KHE) (Kramer 1976; Seifert 2008). This spatial coexistence of crustal and mantle products in distinct upper crustal areas indicates the coincidence of the ascent paths for mafic and granitic melts. The association of lamprophyric intrusions and rare metal granites has been found to be restricted to Paleozoic and Mesozoic orogenic belts of the northern hemisphere (Štemprok and Seifert 2011).

The genetic links between lamprophyre emplacement and origin of late Variscan ore mineralization in the KHE remain poorly understood. While Tischendorf (1986, 1988) did not accept any role of mantle-derived magmas, Kramer (1988) and Seifert (1994) proposed that mafic igneous rocks in the Saxothuringian Zone affected the metallogenetic processes. Lamprophyre (shoshonite) magmas in the Fichtelgebirge–KHE anticlinorium were proposed as possible transport media for volatiles, U, Th, large ion lithophile elements (LILE), and rare and base metals (Kramer and Seifert 1994). In this paper we examine occurrences, mineral assemblages and bulk chemical composition of several lamprophyre types and other mafic dykes in the Krupka Sn–W–Mo ore district in the eastern KHE. These igneous rocks of mantle origin provide evidence for the presence of upper mantle wedge affected by metasomatism from subducted oceanic crust and/or its sedimentary component. The lamprophyres were subsequently affected by greisenization and show peculiar enrichments in LILE and volatiles resembling enrichments observed in highly evolved peraluminous granites.

2. Geological setting

The KHE forms a part of the Saxothuringian Zone in the Variscan belt of Europe, and contains the geological record of two orogenies: Cadomian (570–540 Ma) and Variscan (370–330 Ma) separated by a period of crustal extension and oceanic sedimentation (Linnemann 2008). In the KHE the Proterozoic and Lower Paleozoic volcanosedimentary and intrusive units were metamorphosed and deformed at medium to ultra-high pressure conditions, leading to the formation of para- and orthogneisses, tectonically overlain and surrounded by micaschists and phyllites (Mingram et al. 2004), and intruded by Late Variscan post-collisional granites (Förster et al. 1999; Breiter 2012). The small occurrences of the Upper Carboniferous and Permian sediments rest unconformably on the metamorphic units (Pietzsch 1962). The NE-trending Sub-Erzgebirge Basin is located between the KHE Metamorphic Complex and the Saxonian Granulite Massif, and it mainly hosts Carboniferous and Permian turbidite and siliciclastic sediments as well as rhyolitic and dacitic volcanic rocks. The KHE region was affected by the Cenozoic magmatic activity, which produced isolated lavas, feeding necks or dykes of olivine basalts through phonolites and their rarely preserved, pyroclastic products.

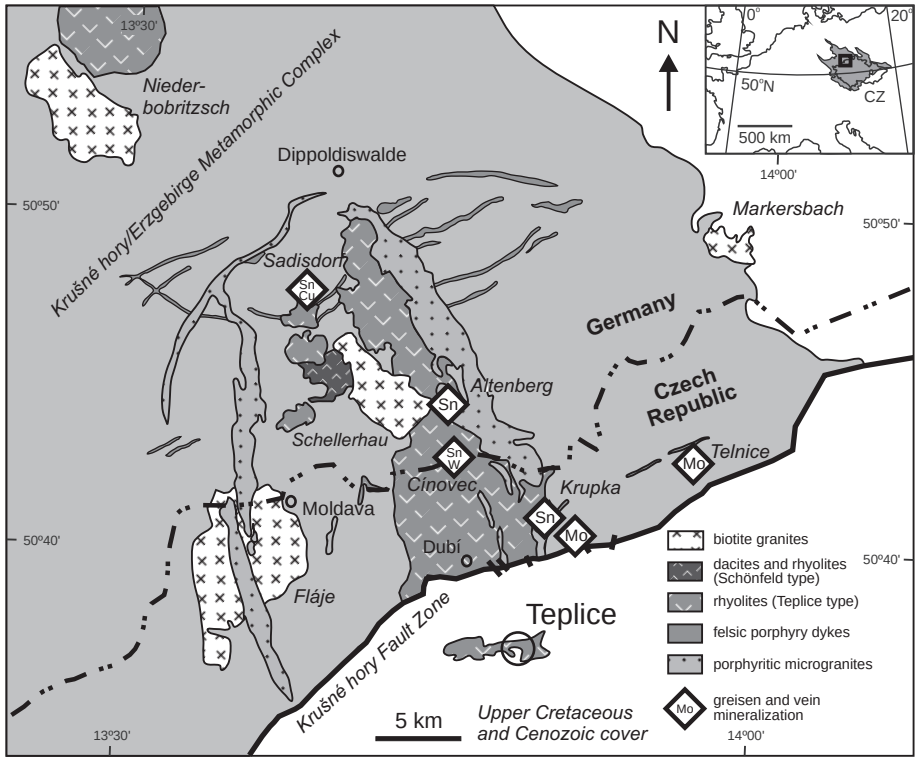

Fig. 1 Geological units of the Eastern KHE and the location of the Cínovec/Zinnwald, Krupka and Altenberg Sn–W–Mo deposits (modified from Wasternack et al. 1995 and Štemprok et al. 2003).

2.1. Variscan magmatic activity in the Eastern KHE

The metamorphic units of the Eastern KHE were intruded by Late Variscan granites, microgranites and rhyolites (predominantly ignimbrites) related to the Altenberg–Teplice Caldera (ATC) (Mlčoch and Skácelová 2010). Magmatic activity commenced with the pre-caldera intrusions of the biotite granites (Fláje, Niederbobritzsch and Telnice massifs, Štemprok et al. 2003) that were emplaced before the formation of the Schönfeld volcanosedimentary unit and the Teplice rhyolite. The Late Variscan igneous products constitute the Eastern Volcano–Plutonic Complex (EVPC) and

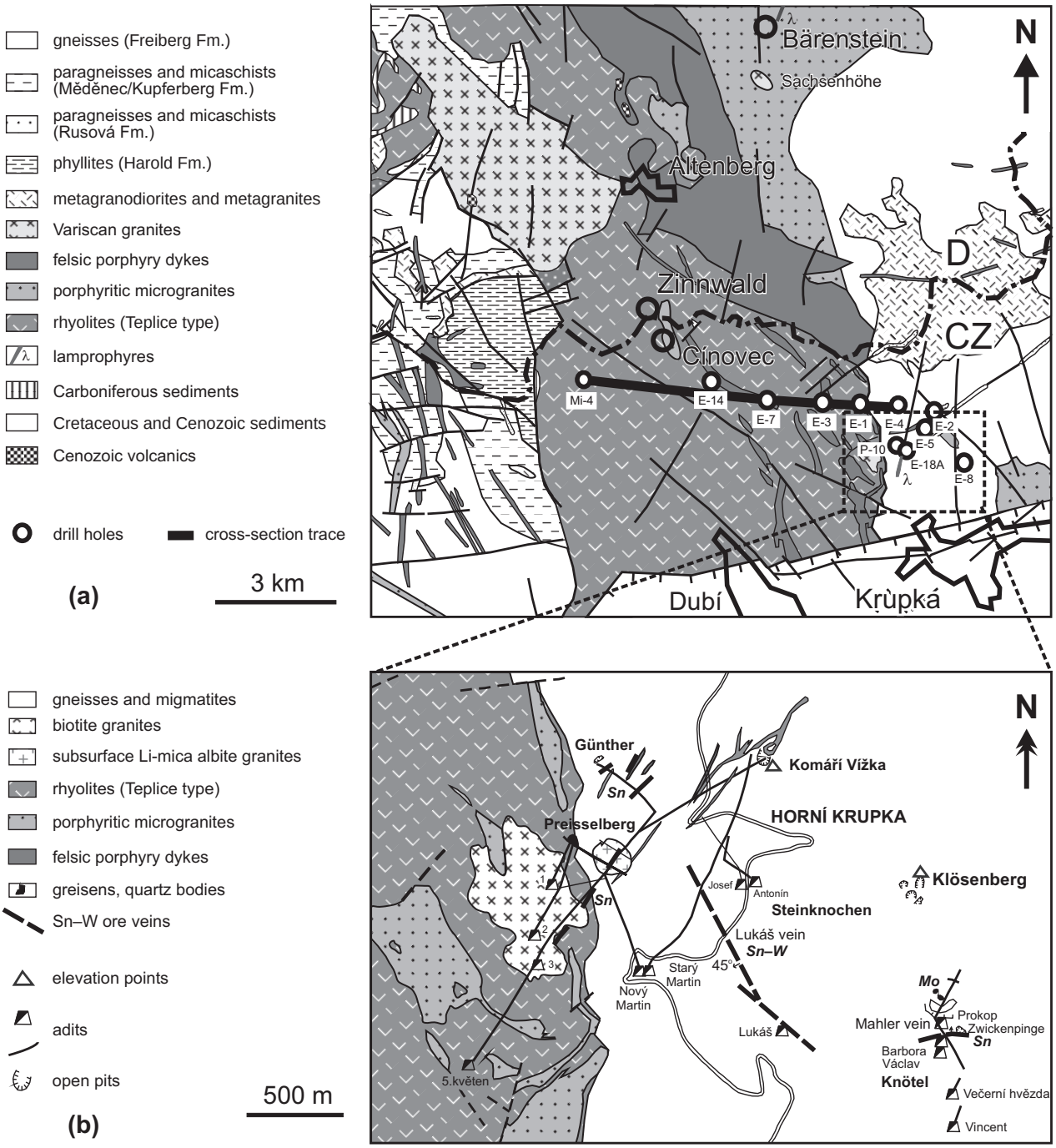

Fig. 2a – geological map of the Cínovec/Zinnwald–Krupka region with the location of the drill holes relevant to this study (modified from Hoth et al. 1994); **b** – detailed geological map of the Krupka ore district with location of the main ore fields and abandoned mine workings (modified from Sejkora and Breiter 1999).

consist of rhyolite and dacite lavas and ignimbrites, and of intrusive bodies of porphyritic microgranites (Müller and Seltmann 2002) originally classified as granite porphyries, and a younger suite of biotite and Li-mica granites (Štemprok et al. 2003; Hoffmann et al. 2013). The granite pluton is only partly exposed. It is subdivided into the Cínovec and Krupka intrusions, which crop out as the Cínovec/Zinnwald, Altenberg, Preisselberg and Schellerhau stocks (Figs 1 and 2). The roof of the pluton between Cínovec and Krupka was examined by numerous exploration drill holes, which revealed generally flat and mildly undulated morphology of the granite upper surface (Chrt and Malásek 1984; Štemprok et al. 1994; Fig. 3). Geochronological data for the Eastern KHE granites, acquired by the U–Pb method, both conventional and LA ICP, Pb–Pb zircon evaporation, Rb–Sr whole-rock, Re–Os molybdenite, Sm–Nd fluorite and K–Ar amphibole or biotite dating, span a range of 327–290 Ma (Förster et al.1999; Romer et al. 2010) but remain problematic especially for the Li-mica granites due to their strong hydrothermal overprint (Gerstenberger 1989). Recent results suggest U–Pb zircon age of 319.2 ± 2.4 Ma for the ATC microgranites (Romer et al. 2010), which is close to the age of the main magmatic event at *c*. 325 Ma in the Western KHE (Kempe et al. 2004; Romer et al. 2007). The ATC developed within two extrusive stages, an early Namurian event at 326.8 ± 4.3 Ma, represented by the Mikulov ignimbrite, and a late caldera-forming event at 308.8 ± 4.9 Ma, recorded by the Teplice rhyolite ignimbrite (Hoffmann et al. 2013). The Li-mica granites at Cínovec/Zinnwald and Krupka (Preisselberg and Knötel granites) intruded the Teplice rhyolite; seven Li-mica separates from granite-derived greisens from Zinnwald yielded Ar–Ar ages between 312.6 ± 2.1 Ma and 314.9 ± 2.3 Ma (Seifert et al. 2011).

Lamprophyre dykes are abundant in the KHE metamorphic units and in the Sub-Erzgebirge Basin. They were subdivided into three suites (Seifert 2008): LD1 kersantites and spessartites, which predated the intrusion of the Eibenstock granite (335–325 Ma); LD2 – mica lamprophyres, which postdated this pluton but were older than the tin–polymetallic mineralization; LD3 – feldspar-phyric "lamprophyres", which were emplaced between the tin–polymetallic mineralization and the Ag-bearing base-metal mineralization. The LD2 and LD3 lamprophyres are associated with a K-rich magmatic event including the A-type felsic intrusions at 315–290 Ma.

In the Eastern KHE area, the lamprophyres occur in the Freiberg polymetallic ± tin vein district and are spatially zoned: kersantites were emplaced in the central part, whereas minettes are more frequent in the south (Baumann et al. 2000; Seifert 2008). Single dykes were described at Sachsenhöhe, south of Bärenstein (minette associated with Sn–W–Bi veins of the greisen type; Fig. 2a), near Bärenstein (spessartite) and at Glashütte, 11 km N of Altenberg (kersantite; Kramer 1976). Lamprophyres in the Krupka district mainly intruded the metamorphic envelope of the Eastern KHE pluton (Eisenreich and Breiter 1993). Single lamprophyre occurrences were described at Knötel and Klösenberg (Fiala 1959), the 5. květen and Nový Martin adits, drill holes E-4, E-18 and E-18A (Pivec et al. 2002; Seifert 2008) (Fig. 2). They are frequently narrowly spaced in dyke swarms. Vertical drill holes intersected numerous lamprophyre dykes of apparent thickness of 0.1–0.7 m, exceptionally up to 15 m (e.g., drill holes E-2 and E-7; Štemprok et al. 2001); some intruded the Teplice rhyolite (drill hole E-3; Chrt and Malásek 1984). Xenoliths of lamprophyre enclosed in the Li-mica alkali feldspar granite were reported from the drill hole E-18 (Štemprok et al. 1994). "Porphyrites" were identified by J. K. Novák (written

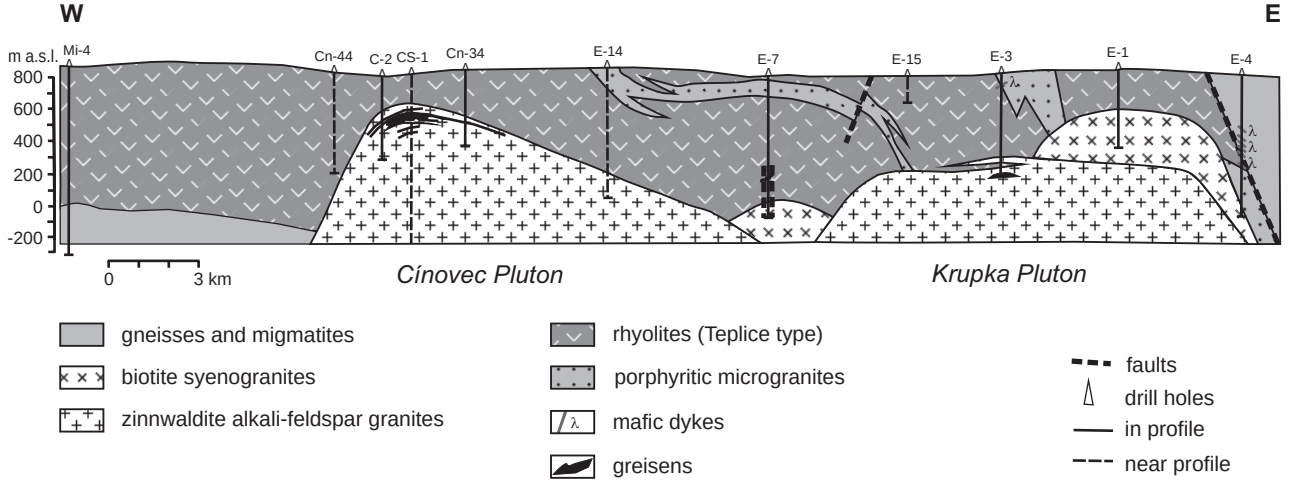

Fig. 3 The W–E geological cross-section through the Cínovec/Zinnwald–Krupka region based on the exploration drill holes (Chrt and Malásek 1984; Štemprok et al. 1994).

communication, 1994) in the drill holes KV-4 (116–124.4 m) and E-7 (622.8–632.0 m) and an altered mafic dyke was investigated in the drill hole E-5 at Komáří Vížka (Pivec et al. 2002). The lamprophyres locally underwent greisenization (drill holes E-4 and P-10 and in the 5. květen adit). A sequence of kersantites and biotite paragneisses *c.* 5–20 m from the rhyolite contact at the Preisselberg district was hydrothermally altered but is devoid of cassiterite mineralization (Janečka and Štemprok 1967). In the drill hole P-10 (Fig. 3), the sequence of kersantite dykes interlayered by gneiss, *c.* 6 m thick, was greisenized and strongly mineralized with cassiterite at the intersection with numerous quartz veinlets, together with some underlying gneisses. The Paleozoic lamprophyres are locally spatially associated with the Cenozoic dykes but can be readily distinguished petrographically.

2.2. Tin–tungsten–molybdenum mineralization of the Krupka district

The Krupka ore district is part of the Late Variscan Sn–W metallogenic province (Eisenreich and Breiter 1993; Novák 1994; Štemprok et al. 1994). The district hosts three main deposits: Cínovec/Zinnwald, Altenberg and Krupka (Fig. 1), controlled by several parallel NW–SE zones, which also carry greisen mineralization (Dalmer 1890; Tischendorf 1963). These zones follow a major NW-trending deep fault zone intersecting the Eastern KHE (Hösel 1972). Among these three deposits, Krupka is the only one which shows the presence of coeval lamprophyre dykes, although lamprophyres also occur at Telnice in association with molybdenum-bearing quartz veins and pyrite mineralization (Gäbert and Beck 1903; Štemprok et al. 2001; Fig. 1).

The Krupka district hosts the greisen mineralization in six ore fields mostly restricted to the contact zone of the hidden or exposed highly evolved granites (Beck 1914; Žák 1966; Eisenreich and Breiter 1993; Štemprok et al. 1994; Sejkora and Breiter 1999; Fig. 2b). The greisen assemblages form lens-like, stockwork and/or vein bodies. The greisen lenses and stockworks consist of quartz, lithium mica and topaz with disseminated cassiterite, wolframite and scheelite. The steeply or gently dipping ore veins are built up by quartz with lesser amounts of lithium mica, topaz and/or alkali feldspar accompanied by cassiterite and wolframite as the principal ore minerals. The veins are irregularly bordered by wall-rock greisens. The highly evolved granite underlying the ore field forms a small, mostly hidden granite stock with a thick "stockscheider", an apical massive feldspar-rich pegmatite body with a molybdenite-bearing quartz core. Lamprophyres occur in a close spatial association with tin- and tungsten-bearing greisens and ore veins near the granite contacts in the Preisselberg and Knötel ore fields and were intersected by mine workings which explored the Sn–W ore bodies.

3. Analytical methods

Twenty-four samples of lamprophyres were collected from exploration trenches, mine dumps, in the adit No. 2 at Preisselberg and from holes drilled by Geoindustria and the Czech Geological Survey in Krupka and the Krupka–Cínovec area. Fifteen samples of lamprophyres and mafic dykes were analyzed for major- and trace-element composition. The samples weighing 0.5–2 kg were crushed and a 30 g aliquot was homogenized in an agate ring mill in the laboratories of the Institute of Geology of the Academy of Sciences of the Czech Republic and the Czech Geological Survey. Major-element concentrations were determined by wet chemical methods at the Czech Geological Survey (Weiss 1983), Institute of Geology of the Academy of Sciences and the Faculty of Science, Charles University. The trace-element concentrations were analyzed by OES (B, Be, Bi, Cu, Ga, Mo, Pb, Sn), XRF (Co, Cr, Ni, Nb, Zr, U), ICP (Hf, REE, Sc, Ta, Th, Y, W) and AAS (As, Ba, Sr, Cs, Rb, V, Zn) at the Czech Geological Survey (Weiss 1983). Concentrations of trace elements in several samples (see Table 2b for details) were measured by AAS (using Varian SpectrAA 200 HT with 0.2 g sample in 100 ml solution), ICP-MS at the Faculty of Science, Charles University (using borate-carbonate fusion (Na_2CO_3 + $Na_2B_4O_7$) with a digestion in HF + $HClO_4$ acid mixture and followed by conventional solution nebulisation in VG PQ3 ICP-MS; Strnad et al. 2005), INAA (Institute of the Nuclear Research, Řež; for analytical details see Mizera and Řanda 2010), ICP-MS at Analytika s.r.o., Prague (using total digestion in HF + $HClO_4$ acid mixture under pressure and determined with the Varian Ultramass instrument) and by XRF at the Department of Lithospheric Research, University of Vienna (using pressed-powder pellets measured with the Philips PW2400 spectrometer). The concentrations of Th and U were also measured by gamma spectrometry (Exploranium CZ, Brno, see Štemprok et al. 2008 for analytical details). The isotopic composition of oxygen was determined by conventional mass spectrometry (Czech Geological Survey, Prague) and presented in Žák et al. (2001).

The electron microprobe analyses of twenty-five samples were performed using the JEOL XA 50A DV 9400 microprobe with energy-dispersive spectrometer at the Institute of Geology of the Academy of Sciences in Prague. Analytical details were given in Pivec et al. (2002). Strongly greisenized lamprophyres were investigated by electron microscopy and microanalysis using the TESCAN Vega scanning electron microscope with

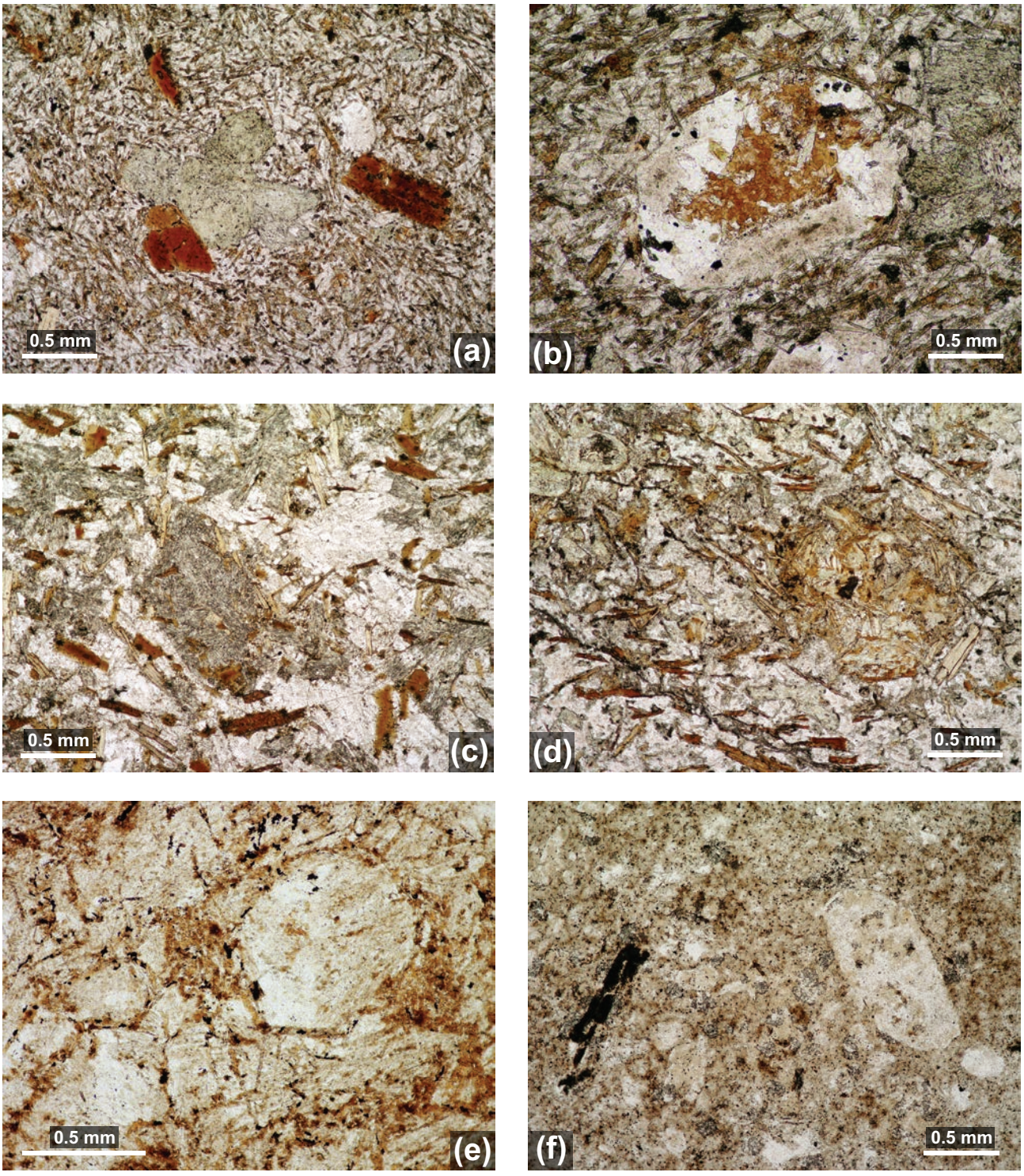

Fig. 4 Photomicrographs of mafic dyke rocks from the Krupka district: **a –** spessartite with phenocrysts of phlogopite and completely uralitized clinopyroxene in a groundmass of acicular hornblende and plagioclase, the Večerní hvězda adit (dump), Knötel ore field, plane polarized light (PPL); **b –** Li-bearing mica infilling the center of a felsic ocellus in spessartite, the Večerní hvězda adit (dump), PPL; **c –** kersantite with carbonatized pilitic and uralitic pseudomorphs after olivine and clinopyroxene, adit No. 2 (dump), Preisselberg ore field, PPL; **d –** minette with uralitized clinopyroxene and pseudomorphs of Mg-rich actinolite and phlogopite after olivine phenocrysts (pilite), drill hole E-4, PPL; **e –** greisenized lamprophyre (spessartite?) with relics of porphyritic and ocellar textures, the 5. květen adit, PPL; **f –** greisenized microdiorite showing plagioclase phenocrysts pseudomorphed by quartz and Li-mica, the Prokop adit (dump), PPL.

the energy-dispersive detector X-Max 50 (Institute of Petrology and Structural Geology, Charles University, Prague). Measurements were carried out with an accelerating voltage of 15 kV, beam current of 1.5 nA and the acquisition time of 100 s.

4. Petrology of mafic dykes

4.1. Spessartites

Spessartite from the Večerní hvězda adit (mine dump) in the Knötel field contains abundant phenocrysts of completely uralitized clinopyroxene and less abundant red-brown phlogopite up to 2 mm across (Fig. 4a). Rare pilite clusters of Mg-rich actinolite ± phlogopite are interpreted as pseudomorphosed original olivine phenocrysts (0.5–1 mm). The groundmass is dominated by acicular brown amphibole (potassian titanian magnesiohastingsite according to Leake et al. 1997) and prismatic to poikilitic plagioclase $An_{35–50}$. Quartz is rare. The rock hosts small (commonly < 1 mm) ocelli of felsic minerals (plagioclase prevails over quartz), in places with subordinate Mg-rich actinolite or clusters of fine-grained Li-bearing dark mica with orange-brown pleochroic colours (Y, Z) (Fig. 4b). This mica variety is also present in irregular spots in the groundmass where it partly replaces all original minerals. Accessory minerals are dominated by apatite with subordinate amounts of titanite, chromite, magnetite, pyrrhotite and leucoxene aggregates.

4.2. Kersantites

Former clinopyroxene phenocrysts, locally clustered and sometimes with well-preserved original crystal shapes, were completely replaced by uralite pseudomorphs. Rare phenocrysts of olivine were altered to phlogopite–actinolite aggregates. Red-brown phlogopite phenocrysts are optically unzoned and highly variable in size (up to 4 mm) with seriate size distribution. The groundmass (0.15–0.6 mm) of kersantites consists of phlogopite, Mg-rich actinolite (replacing clinopyroxene or surrounding biotite), plagioclase ($An_{32–50}$) and subordinate amounts of K-feldspar and quartz in some samples. Accessory minerals are represented by apatite, titanite (leucoxene), minute crystals of chromite in pilitic pseudomorphs and irregularly distributed sulphides. Kersantite samples from the Preisselberg ore field and from the drill hole E-8 (Fig. 2) contain uralitic and pilitic pseudomorphs that were largely transformed to carbonate, which mimics the shape of aggregates of actinolite needles (Fig. 4c). The common presence of very fine-grained secondary biotite and rare aggregates of orange lithium-bearing mica suggests an incipient greisen alteration. Other secondary minerals are represented by rare chlorite, epidote, carbonate, sericite and clay minerals.

4.3. Minettes

Minettes from the E-4 and E-18A boreholes are characterized by abundant phenocrysts of phlogopite, uralitized clinopyroxene and pilitic clusters replacing the former olivine (Fig. 4c,d). Some samples contain rare xenocrysts of quartz. Phlogopite is only weakly zoned, frequently kinked and it lacks mostly the typical euhedral habitus, characteristic of many minettes elsewhere (Rock 1991). The uralitic pseudomorphs commonly preserve crystal shapes of original clinopyroxene and frequently occur in clusters. The pilitic pseudomorphs up to 2 mm in size consist of small nearly colourless Mg-rich actinolite grains or needles intergrown with abundant phlogopite and minute grains of accessory magnetite, chromite and sulphides. The groundmass (up to 0.3 mm), with occasional weak mineral orientation, is composed of small phlogopite flakes, abundant Mg-rich actinolite (after clinopyroxene) and very fine-grained K-feldspar with some quartz. The most common accessory minerals restricted to the groundmass are apatite and titanite, whereas magnetite is very rare. Columnar to acicular apatite is cloudy and pleochroic (greyish to yellowish brown transversely *vs*. dark or pinkish grey along the *c* axis) due to the presence of an extremely fine pigment.

The minette samples from the 5. květen and Nový Martin adits (dumps) contain, in addition, actinolite clusters that only rarely preserve the shapes of original mafic phenocrysts. The groundmass contains fans of laths and, rarely, imperfect spherulitic aggregates of K-feldspar. The presence in some samples of dispersed extremely fine flakes of brown to brownish-yellow secondary dark mica suggests an incipient greisen alteration. Carbonate veinlets (siderite at the margin and calcite in the interior) postdated the greisen alteration. Chlorite and epidote are generally rare and not present in all samples.

4.4. Microdiorites

A mafic dyke NE of Klösenberg, originally classified as biotite porphyrite (Fiala 1959), contains biotite and untwinned oligoclase–andesine phenocrysts scattered in a groundmass of very fine-grained biotite, quartz, plagioclase, apatite and magnetite. We have identified similar, strongly altered, nearly vertical dyke in the drill hole E-5 where it crosscuts the biotite microgranite. The original plagioclase microphenocrysts (0.2–0.8 mm) were replaced by carbonate ± quartz pseudomorphs. The groundmass (0.01–0.2 mm) contains brown dark mica, quartz and minute opaque minerals. Accessory miner-

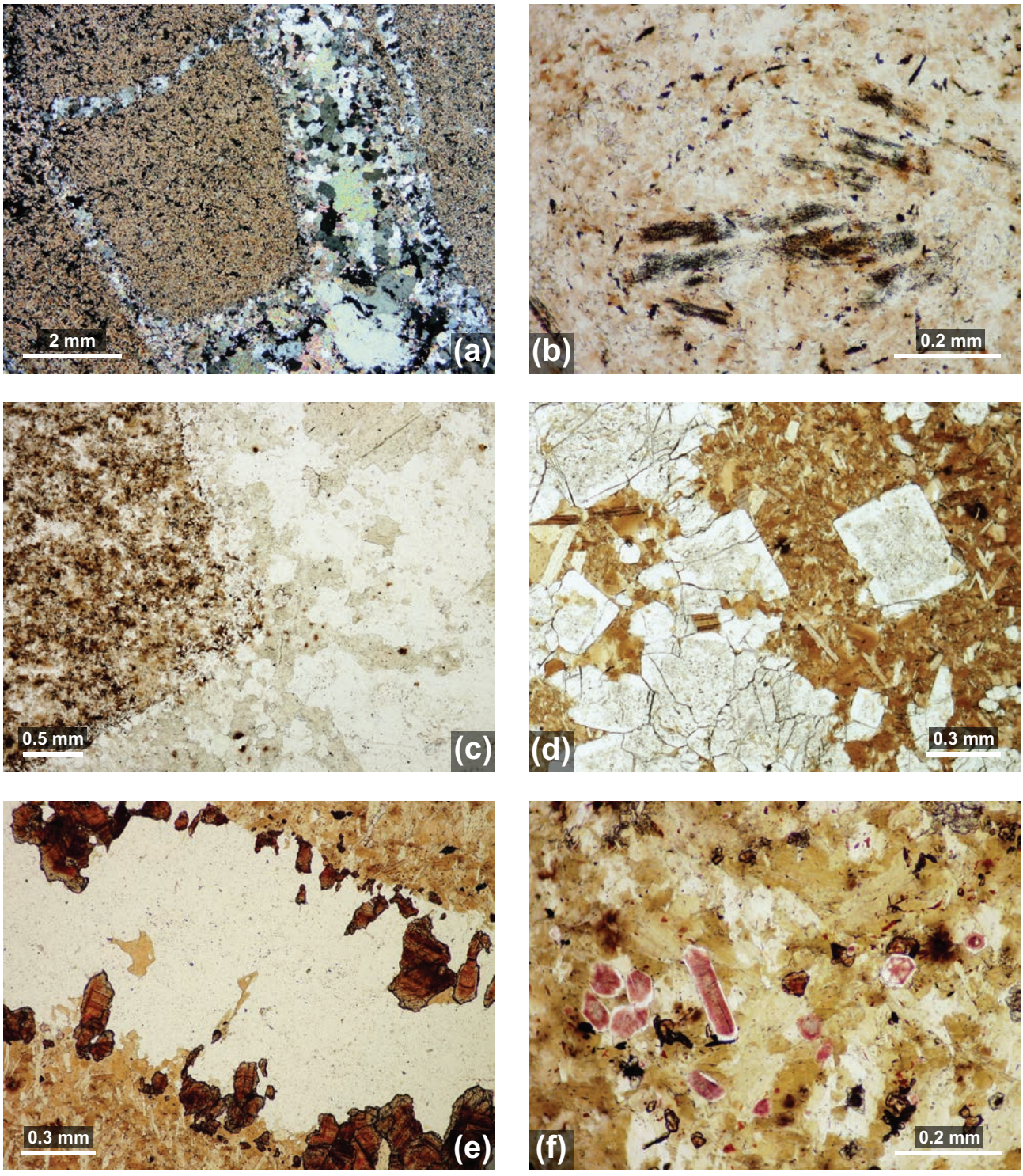

Fig. 5 Photomicrographs of strongly greisenized lamprophyres and associated rocks: **a –** greisenized aplite veinlet intersecting the greisenized lamprophyre. Altered aplite consists of crystals of Li-mica in a quartz–topaz aggregate, greisenized lamprophyre is fine-grained Li-mica glimmerite with rare topaz and fluorite, the Večerní hvězda adit (dump), Knötel ore field, crossed nicols; **b –** greisenized lamprophyre with biotite altered to Li-mica accompanied by rutile (sagenite), the Večerní hvězda adit (dump), PPL; **c –** two contrasting varieties of mica in the breccia: brownish dark mica in greisenized lamprophyre and greenish zinnwaldite in greisenized aplite, the Večerní hvězda adit (dump), PPL; **d –** topaz–mica rock, probably a strongly greisenized paragneiss associated with the greisenized lamprophyre, drill hole P-10, depth 106.7 m, PPL; **e –** greisenized lamprophyre with quartz veinlet containing cassiterite at margins, drill hole P-10, depth 112.6 m, Preisselberg ore field, PPL; **f –** greisenized lamprophyre containing dispersed cassiterite crystals in a Li-mica aggregate, apatite crystals with red-cloudy cores and light outer rims, drill hole P-10, depth 111.6 m, PPL.

als are apatite, ilmenite (leucoxene aggregates), skeletal crystals of sulphides and hematite.

4.5. Greisenized lamprophyres and microdiorite

Greisen alteration of fresh lamprophyres first appears in pseudomorphs after olivine and in some parts of the groundmass. In spessartite from the Večerní hvězda adit, irregular dark spots in the groundmass are formed by fine-grained orange lithian phlogopite. In addition, the Li-bearing dark mica may also replace some inner parts of felsic ocelli (Fig. 4b). Some lamprophyre samples (e.g., from the drill hole P-10 or the 5. květen adit) display minute flakes of lithium dark mica replacing the feldspar-rich groundmass. Primary biotite phenocrysts are replaced by fine aggregates of lithium-rich mica (0.3–0.5 mm).

Strongly greisenized mafic dykes consist of a fine-grained mixture of brownish dark mica and quartz accompanied by variable amounts of fluorite. Accessory minerals are apatite, titanium oxides and minute grains of opaque radioactive minerals. Original texture is commonly preserved as relics – larger flakes, which contain secondary titaniferous minerals, presumably represent original phlogopite phenocrysts. Local variations in fine-grained secondary micas possibly record outlines of former phenocrysts and perhaps of ocelli (Fig. 4e). The strongly greisenized mafic rock (LA 159) from the Prokop adit (dump), also composed of brownish mica, quartz and minor fluorite, shows, by contrast, relict porphyritic texture with well-preserved shapes of small (0.3–1.5 mm) plagioclase phenocrysts, now replaced by aggregates of quartz and lithium-bearing mica, and less abundant phenocrysts of biotite (with disseminated secondary titanium oxides) (Fig. 4f). These textural features argue for the microdiorite (diorite porphyry) precursor similar to that described by Fiala (1959).

Several occurrences of magmatic breccia at the Večerní hvězda and Prokop adits (mine dumps) with lamprophyre xenoliths enclosed in aplitic or microgranitic rock or veined matrix provide additional examples of greisen alteration imposed on different precursors (Fig. 5a). The altered lamprophyre is dominated by very fine-grained (0.01–0.1 mm) pale brown to yellowish-brown lithian phlogopite. Sagenite grids attest to the replacement of original titaniferous phlogopite phenocrysts up to 0.5 mm in size (Fig. 5b). The greisen alteration in aplite leads to the formation of quartz-rich assemblage. The dark mica is zinnwaldite (0.05–1.5 mm), which is very pale and greenish-tinged, with brown pleochroic haloes (Fig. 5c) accompanied by topaz and fluorite.

Extremely strong greisenization of lamprophyres leads to the formation of massive dark grey greisens observed in the drill hole P-10 in the Preisselberg ore field (Fig. 5d). A lamprophyre dyke is crosscut by up to 5 mm thick cassiterite-bearing quartz veinlets surrounded by discontinuous selvages of light orange-brown lithian biotite with disseminated fluorite and topaz. Fine (0.1–0.5 mm) grains of optically zoned cassiterite are found near margins of some veinlets (Fig. 5e), whereas elsewhere fluorite becomes abundant but cassiterite is lacking. A conspicuous alteration zoning was observed across the contact between the greisenized lamprophyre and a cassiterite-bearing quartz veinlet. The outer exocontact zone, formed by glimmerite, mainly consists of phlogopite, fluorite, quartz and topaz. The inner exocontact zone, adjacent to the veinlet, is enriched in lithian phlogopite (in the form of larger flakes), cassiterite, scheelite and apatite, but depleted in quartz, topaz and fluorite (Novák et al. 2001).

The original petrographic nature of strongly greisenized mafic rocks is almost completely obscured by newly formed minerals. The alteration products are dominated by lithium-bearing dark mica of variable grain size (0.1–7 mm), with smaller amounts of fluorite (irregular grains with abundant inclusions of mica), apatite, cassiterite, titanium-bearing minerals and minute grains of a radioactive mineral as indicated by dark brown pleochroic haloes when enclosed in mica. Columnar apatite crystals are optically zoned, with reddish grey- to red-cloudy interior and colourless rims (Fig. 5f). The very fine red pigment is apparently oxidized compared to the cloudy apatite in fresh or weakly altered minettes, whereas the clear rims may represent secondary overgrowths during hydrothermal remobilization of phosphorus.

The strongly greisenized lamprophyres in the drill hole P-10 are spatially associated with metasomatic topaz-rich glimmerites (e.g., at 106.7 m depth; Fig. 5d). In addition to zinnwaldite, they contain topaz, fluorite and accessory cassiterite. The abundance of topaz (20–45 vol. %), lack of apatite and, in particular, the presence of small round zircon grains corresponding in size and shape to those in surrounding paragneisses argue for their origin by extreme greisen alteration of country rocks rather than of lamprophyres. The petrographic investigation thus indicates that the greisenized rock sequence in the interval of 106.2–114.0 m of the drill hole P-10, originally described as a single kersantite dyke (Janečka and Štemprok 1968), was formed by replacement of a paragneiss suite crosscut by several lamprophyre dykes, which is underlain by weakly greisenized paragneiss (114.0–120.0 m depth).

5. Chemical composition of dark micas

Dark micas represent characteristic and ubiquitous products of magmatic crystallization and hydrothermal

Tab. 1 Representative chemical compositions and crystallochemical formulae of dark micas

Rock type	Mi	Mi	Ke	Ke	Ke	Ke	Ke	Sp	Di	Di	GL	GL
Sample	LA131	LA167	LA107	LA108	LA109	LA113	LA170	LA119	LA117	LA139	LA154	LA165
SiO_2 (wt. %)	37.01	37.33	36.04	34.53	35.00	39.24	35.55	37.15	36.49	36.81	38.14	38.11
TiO_2	5.15	2.65	5.80	4.83	5.14	1.86	2.57	3.47	2.37	2.30	1.74	2.07
Al_2O_3	15.49	13.69	15.80	16.55	16.56	13.76	16.28	14.17	15.99	18.41	14.28	14.64
Cr_2O_3	0.15	1.00	0.17	–	0.19	0.19	0.20	0.47	–	–	0.05	0.55
FeO	12.90	13.98	11.53	15.33	12.76	14.91	15.81	15.57	17.37	16.53	16.06	15.88
MnO	0.21	0.25	0.25	0.32	0.31	0.35	0.21	0.35	0.28	0.44	0.29	0.29
MgO	14.63	15.89	15.78	12.93	14.51	14.95	14.26	14.04	13.38	11.24	13.85	13.42
CaO	0.15	0.18	0.24	0.31	0.22	0.11	0.05	0.14	0.11	0.21	0.14	0.27
BaO	–	0.15	–	0.81	0.46	–	0.41	0.29	–	–	0.39	0.33
Li_2O*	0.48	0.50	0.39	0.43	0.57	0.34	0.38	0.33	0.21	0.42	0.46	0.83
Na_2O	0.63	0.67	0.34	0.57	0.45	0.74	0.46	0.65	0.53	0.27	0.72	0.64
K_2O	9.25	9.33	9.22	8.96	9.49	9.18	9.58	8.97	9.32	9.23	9.06	9.31
H_2O†	3.67	3.42	3.61	3.40	3.24	3.99	3.43	3.23	3.69	4.03	3.43	3.74
F	0.87	1.17	0.93	1.20	1.67	–	1.08	1.56	0.63	–	1.06	0.52
Cl	–	0.17	0.09	–	–	0.19	0.17	0.11	–	–	0.23	0.18
Total	100.22	99.85	99.78	99.67	99.87	99.77	99.95	99.82	100.11	99.89	99.40	100.52
Si (apfu)	2.719	2.784	2.651	2.606	2.604	2.912	2.675	2.786	2.740	2.740	2.869	2.832
$Al^{[4]}$	1.281	1.203	1.349	1.394	1.396	1.088	1.325	1.214	1.260	1.260	1.131	1.168
$Al^{[6]}$	0.060	–	0.020	0.078	0.056	0.115	0.119	0.039	0.154	0.354	0.135	0.114
Ti	0.285	0.149	0.321	0.274	0.288	0.104	0.145	0.196	0.134	0.129	0.098	0.116
Cr	0.009	0.059	0.010	–	0.011	0.011	0.012	0.028	–	–	0.003	0.032
Fe	0.793	0.922	0.709	0.968	0.794	0.925	0.995	0.977	1.091	1.029	1.010	0.967
Mn	0.013	0.016	0.016	0.020	0.020	0.022	0.013	0.022	0.018	0.028	0.018	0.018
Mg	1.602	1.767	1.730	1.455	1.609	1.654	1.600	1.570	1.498	1.563	1.553	1.487
Li	0.141	0.150	0.115	0.132	0.171	0.100	0.116	0.100	0.063	0.126	0.140	0.246
$□^{[6]}$	0.098	–	0.079	0.073	0.052	0.069	–	0.069	0.043	0.087	0.042	–
Ca	0.012	0.014	0.019	0.025	0.018	0.009	0.004	0.011	0.009	0.017	0.011	0.021
Na	0.090	0.097	0.048	0.083	0.065	0.106	0.067	0.095	0.077	0.039	0.105	0.092
K	0.867	0.888	0.865	0.862	0.901	0.869	0.920	0.858	0.893	0.876	0.869	0.883
$□^{[12]}$	0.032	–	0.068	0.005	0.003	0.016	–	0.027	0.021	0.068	0.003	–
OH	1.798	1.703	1.772	1.714	1.607	1.976	1.721	1.616	1.850	2.000	1.719	1.855
F	0.202	0.276	0.216	0.286	0.392	–	0.257	0.370	0.150	–	0.252	0.122
Cl	–	0.021	0.011	–	–	0.024	0.022	0.014	–	–	0.029	0.023

Rock types: Mi – minette, Ke – kersantite, Sp – spessartite, Di – microdiorite, GL – greisenized lamprophyre
* calculated (see text for detailed explanation)
† calculated from stoichiometry

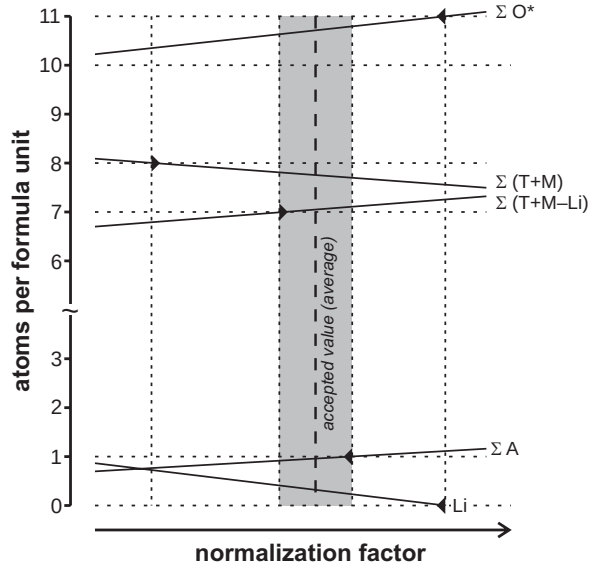

Fig. 6 Diagram of normalization factor (moles per 100 g rock to formula unit per 11 O) *vs.* number of atoms illustrating the chemical and crystallochemical constraints, which limit the permissible normalization range and the lithium concentration. Symbols for site occupancies: A – interlayer, M – octahedral, T – tetrahedral. $O^* = O – Li/2$.

greisenization in lamprophyres. Since greisenization is associated with significant addition of lithium that cannot be determined by electron microanalysis, an independent procedure for estimation of the Li concentration must be used. Tindle and Webb (1990) and Tischendorf et al. (1997, 2004) proposed simple correlation relationships that allow estimation of Li contents based on SiO_2, MgO or F concentrations, applicable to various types of intrusive rocks. Application to greisenized lamprophyres in this study revealed that several these calibrations provided widely different results (0–5.9 wt. % Li_2O) that did not correlate with optical properties (pleochroism) and frequently violated crystallochemical constraints such as

site occupancies. This indicates that the available correlation formulae severely under- or overestimate permissible lithium concentrations.

We utilized recalculation procedure that continuously varied the total number of cations (except for Li) from ~5 to 8, in the sense of Schumacher (1997), and calculated the lithium concentration by charge balance to satisfy 11 oxygen atoms. Concentrations of all cations thus change continuously but are bracketed by the following chemical and crystallochemical limits: (i) $Li \geq 0$, (ii) $2 \leq \Sigma M^{[6]} \leq 3$, and (iii) $\Sigma M^{[12]} \leq 1$ (Fig. 6). These three constraints must be satisfied simultaneously and they provide rather narrow brackets for normalization factors and Li concentrations. We used an arithmetic average between the minimum and maximum bracket for the resulting formula unit (see Schumacher 1997; Fig. 6).

The dark micas in lamprophyres and their greisenized varieties range from primary titaniferous phlogopite to secondary Ti-depleted lithian phlogopite (Tab. 1; Fig. 7). The micas contain 26.9–31.3 wt. % MgO + FeO_{tot}, 13.8–18.4 wt. % Al_2O_3, 1.42–5.89 wt. % TiO_2, 0.08–1.16 wt. % Li_2O and up to 4.17 wt. % F. The total Al concentrations range from 0.4 to 1.6 apfu, with the

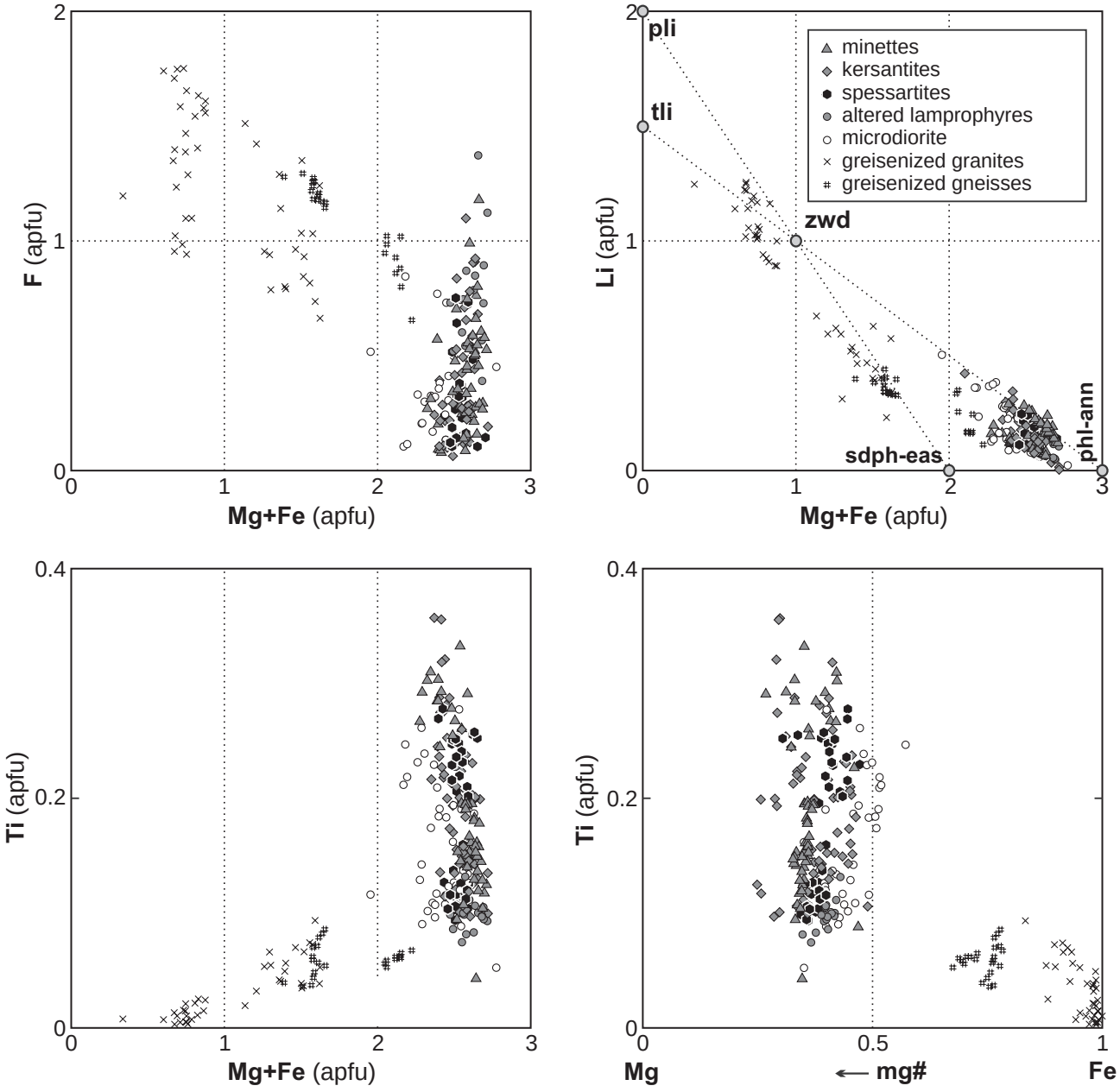

Fig. 7 Chemical composition of dark micas from fresh and greisenized mafic dykes, greisenized paragneisses and granite greisens. Mineral abbreviations: ann – annite, eas – eastonite, phl – phlogopite, pli – polylithionite, sdph – siderophyllite, tli – trilithionite, zwd – zinnwaldite.

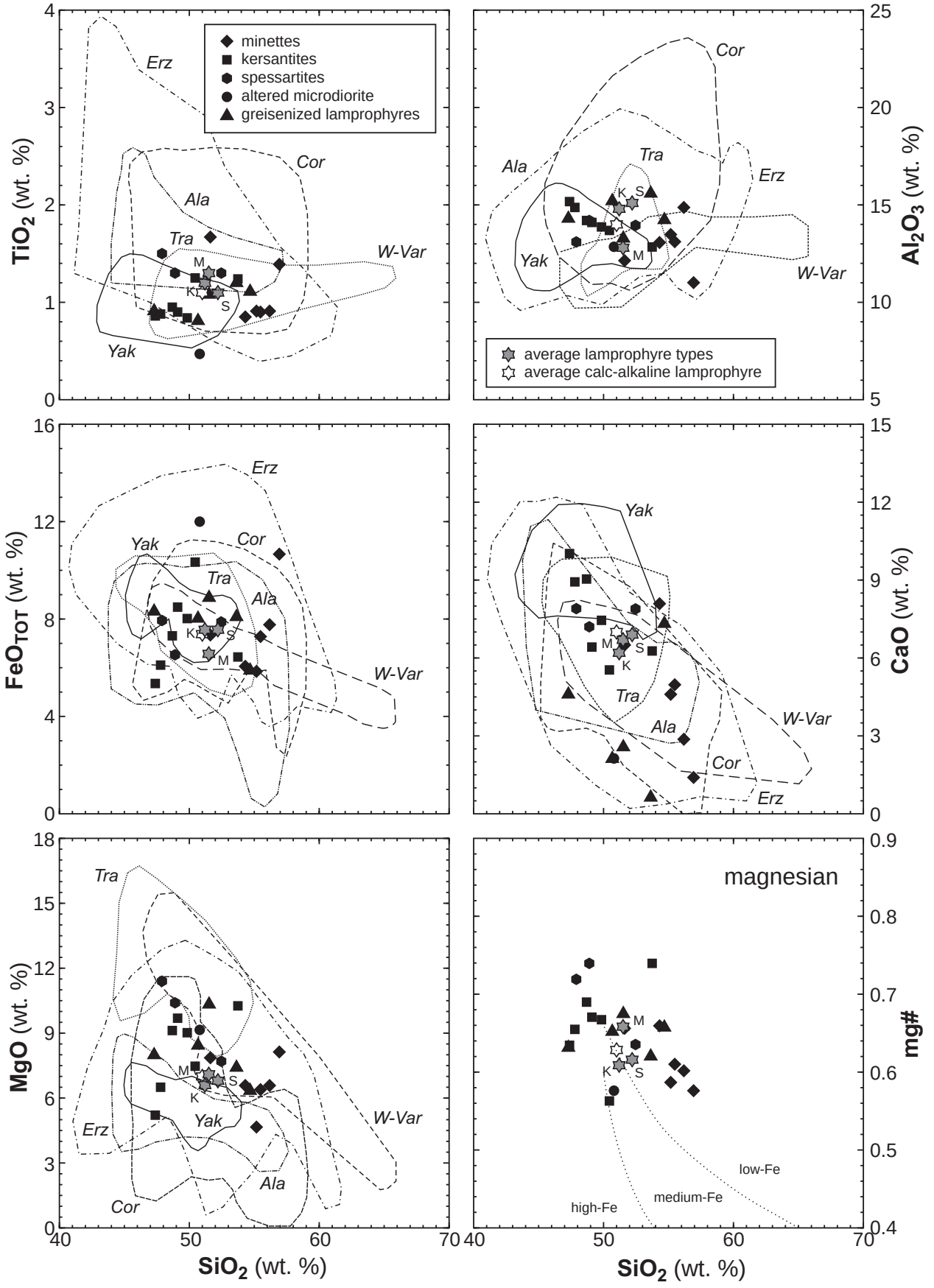
minettes
kersantites
spessartites
altered microdiorite
greisenized lamprophyres
average lamprophyre types
average calc-alkaline lamprophyre
Erz
Cor
Ala
Tra
W-Var
Yak
M
K
S
TiO2 (wt. %)
Al2O3 (wt. %)
FeOTOT (wt. %)
CaO (wt. %)
MgO (wt. %)
mg#
SiO2 (wt. %)
magnesian
low-Fe
medium-Fe
high-Fe

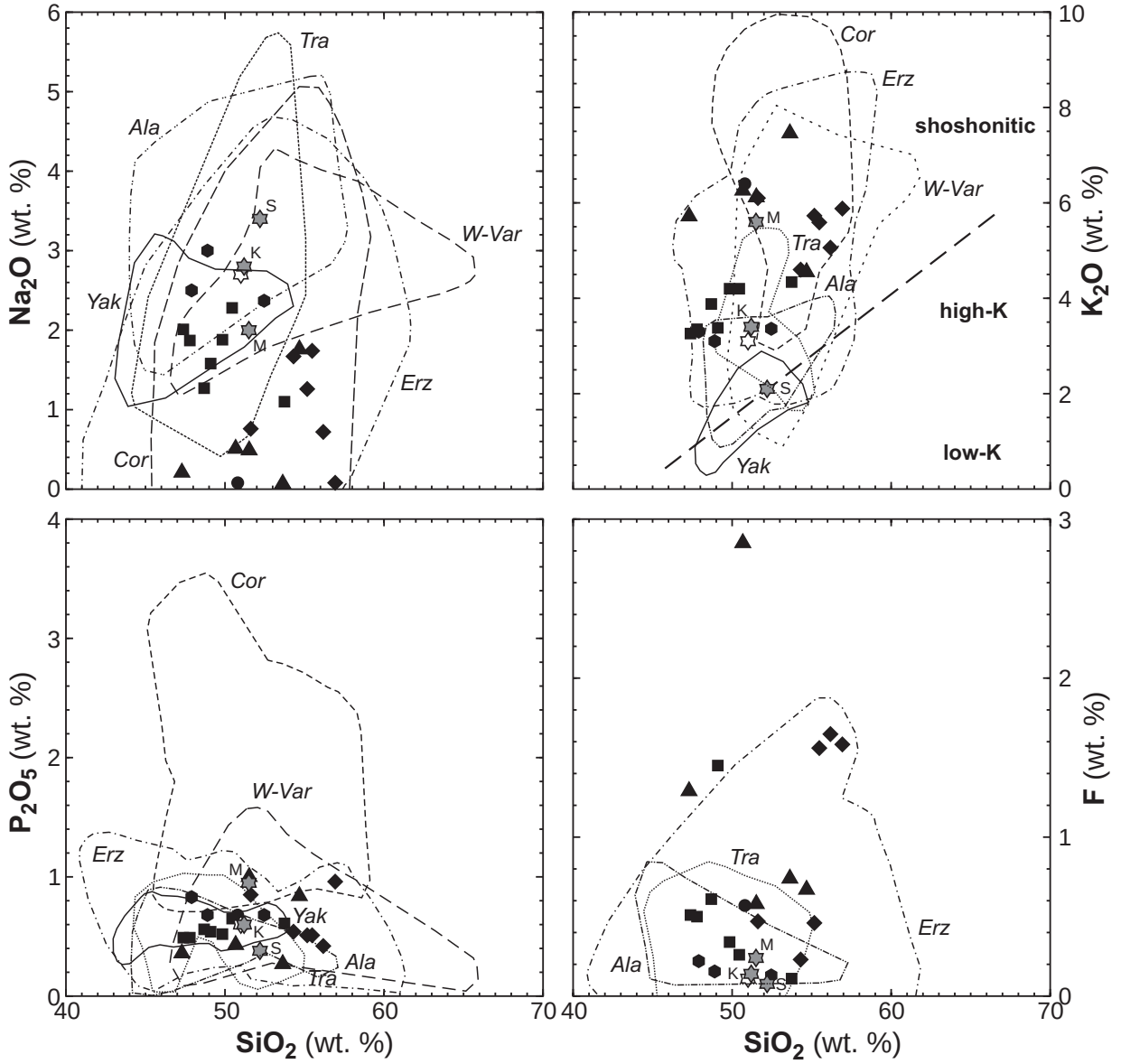

Fig. 8 Harker variation diagrams for the lamprophyres and other mafic rocks from the Krupka district (Tab. 2; Štemprok et al. 1994; Seifert 2008) and their comparison with lamprophyre compositions from representative districts with rare metal mineralization. Symbols for average calc-alkaline lamprophyres (Rock 1991): K – kersantite, M – minette, S – spessartite. Abbreviations: Ala – Alaska (Sainsbury 1968; Sainsbury et al. 1967); Cor – Cornwall (Fortey 1992); Erz – KHE (Kramer 1976; Seifert 2008); Tra – Transbaikalia (Troshin 1978; Abushkevich and Syritso 2005, 2007); W-Var – Western European Variscides (Turpin et al. 1988); Yak – Yakutia (Korostelev 1977). The lamprophyres from Krupka belong to the magnesian igneous rocks using the criteria of Frost and Frost (2008) but cannot be uniquely classified in the previous classification of Arculus (2003).

octahedral occupancy up to 0.16 vacancies pfu and the mg# values, i.e., the molar MgO/(MgO + FeO_{tot}) ratio, from 0.48 to 0.76. Replacement and new formation of micas during greisen alteration is characterized by a significant loss of titanium (from 0.36 to 0.08 Ti apfu), a weak enrichment in lithium (up to 0.3, rarely 0.5 Li apfu) and a strong addition of fluorine (from 0.10 to 1.35 F apfu). The incorporation of lithium was facilitated by the intraoctahedral coupled substitution $LiAl(Mg,Fe)_{-2}$ as indicated by the location of the analyzed micas along the phlogopite–zinnwaldite join (Fig. 7). The lithium addition is interpreted to reflect the chemical signature of the greisenizing fluids. The Ti loss from mica during greisen alteration has been balanced by the addition of Mg and Fe in the octahedral site by the exchange vector of $(Mg,Fe)_2Ti_{-1}$. The titanium loss was probably related to low temperature of hydrothermal replacement because incorporation of Ti into dark micas is strongly temperature-dependent (Luhr et al. 1984; White et al. 2007; Tajčmanová et al. 2009).

6. Whole-rock geochemistry

6.1. Major- and trace-element composition

The SiO_2 concentrations in the investigated lamprophyres range from 47 to 56 wt. % SiO_2 but, in detail, they differ for kersantites (47.4–50.5 wt. %) and minettes (51.6–56.2 wt. %), whereas the single SiO_2 value for spessartite (52 wt. %) is within the range of minettes (Tab. 2a; Fig. 8; Kramer 1976; Štemprok et al. 1994; Novák et al. 2001; Seifert 2008). In the $Na_2O + K_2O$ *vs.* SiO_2 diagram the Krupka lamprophyres straddle the boundary between alkaline and subalkaline domains and correspond to shoshonites, with overlap to potassic trachybasalts and latites (Fig. 9).

The Al_2O_3 and TiO_2 concentrations are low and variable (12.14–15.20 and 0.81–1.67 wt. %, respectively), with the Al_2O_3/TiO_2 ratio of 7.3–18.8, which supports the lamprophyre origin in a subduction rather than within-plate setting (Müller et al. 1992; Müller and Groves 1993). The MgO contents decrease from 10.33 to 4.66 wt. % as do the FeO_{TOT} abundances (11.99–5.35 wt. %). The mg# values, molar $MgO/(MgO + FeO_{tot})$ ratio, range from 0.74 to 0.56 and indicate that the lamprophyres represent primary mantle-derived melts, which experienced limited if any fractionation and/or crustal contamination. The CaO abundances are very variable (2.12–10.02 wt. %), higher in kersantites than in minettes. Both the CaO and Na_2O concentrations sharply decrease during greisenization due to the decomposition of feldspars. Minettes are distinctly enriched in potassium (4.6–6.10 wt. % K_2O) in comparison with kersantites (3.26–4.20 wt. % K_2O). With progressive greisen alteration, the K_2O concentrations further increase (6.10–7.46 wt. % K_2O) due to the formation of lithium micas; none of these greisenized samples is sodic. All but two fresh lamprophyres can be classified as ultrapotassic and shoshonitic magmas using the criteria of Foley et al. (1987). The P_2O_5 contents range between 0.42 and 0.85 wt. %, and the fluorine concentrations exhibit a wide range (0.11–1.65 wt. %, with one sample at 2.85 wt. %), including enrichment in apparently unaltered lamprophyres (to ~1.65 wt. % F), comparable to other occurrences in the KHE (Kramer 1976). The CO_2 contents are elevated up to 5.39 wt. % and they record the variable presence of carbonates as the products of hydrothermal alteration of lamprophyres.

The concentrations of compatible elements in the Krupka lamprophyres are high (348–580 ppm Cr, 129–366 ppm Ni, 12–36 ppm Sc, 18–50 ppm Co; Fig. 10). The abundances of Cr and Ni suggest that they are primary melts that have not undergone any significant crystal fractionation or contamination by evolved crustal material. The V concentrations are elevated (132–176 ppm), and this is reflected in the low Ti/V ratios (39.9–56.7 by weight) characteristic of alkaline magmas.

The Zr contents range between 315 and 678 ppm, while most Hf concentrations are close to 17 ppm. These elevated abundances may be hosted by titanite (Seifert and Kramer 2003). The Nb concentrations range between 10 and 45 ppm, which conforms with the origin of potassic lamprophyres in orogenic setting (Bianchini and Wilson 1999; Semiz et al. 2012).

The Th concentrations are high (17–66 ppm), and this enrichment is characteristic of the lamprophyres from the Jáchymov ore district in the Western KHE (Štemprok et al. 2008). It appears to be a general feature of the Variscan lamprophyres in central Europe (Seifert 2008; Abdelfadil et al. 2013). The U concentrations vary from 6 to 29 ppm and are likewise higher than the average concentration in lamprophyres worldwide

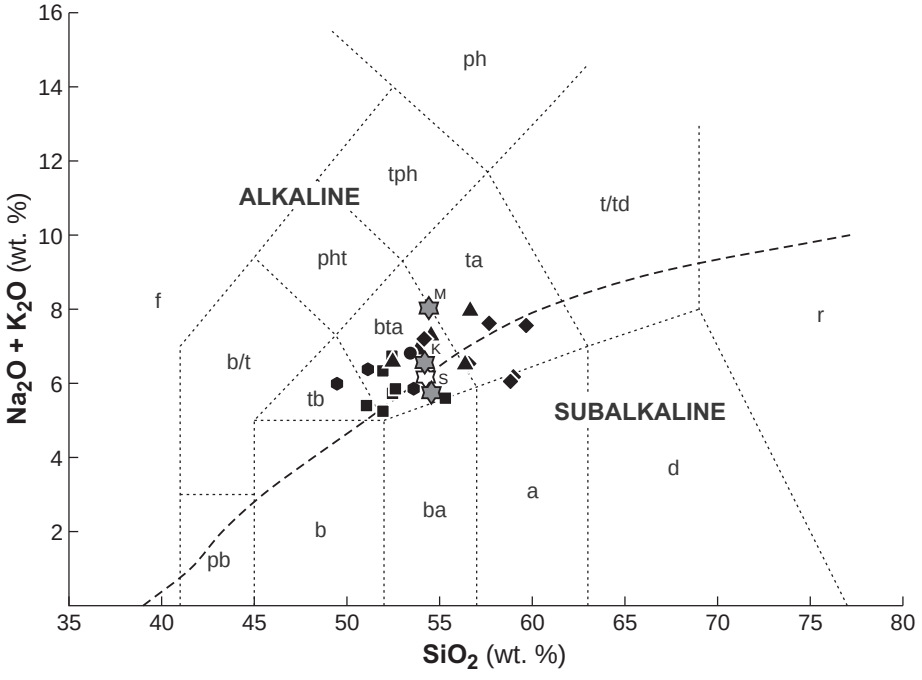

Fig. 9 Total alkali *vs.* silica diagram (Le Maitre 2002) with subdivision for alkaline and subalkaline rock series (Irvine and Baragar 1971). Abbreviations: a – andesite, b – basalt, ba – basaltic andesite, b/t – basanite or tephrite, bta – basaltic trachyandesite, d – dacite, f – foidite, pb – picrobasalt, ph – phonolite, pht – phonotephrite, r – rhyolite, ta – trachyandesite, t/td – trachyte or trachydacite, tph – tephriphonolite. Symbols are as in Fig. 8.

Tab. 2a Chemical composition of mafic dyke rocks from the Krupka ore district (major and minor components)

	1	2	3	4	5	6	7	8	9	10	11	12	13	14	15	16
Sample	E-4-21	E-18A-25	E-18A-29	Vr-626	Kr-626	E-18A-8	G2-2119	PrG2-PI2	PrG2-19	LA161	LA170	LA162	E-4-18	P-12-159	E-4-37	E-5-57
Rock	Mi	Mi	Mi	Mi	Mi	Ke	Ke	Ke	Ke	Ke	Ke	Sp	GL	GL	GL	Di
SiO_2 (wt. %)	54.31	55.17	55.48	51.62	56.18	48.69	47.79	47.38	49.10	50.45	49.84	52.46	51.52	50.67	53.63	50.80
TiO_2	0.85	0.91	0.90	1.67	0.91	0.95	0.88	0.86	0.90	1.25	0.84	1.30	1.08	0.81	1.20	0.94
Al_2O_3	13.07	13.48	13.11	12.14	14.87	14.20	14.87	15.17	14.10	13.69	13.87	13.95	13.28	15.20	15.59	12.85
Fe_2O_3	0.92	1.21	1.01	2.47	8.63*	1.30	1.53	1.38	1.81	1.62	1.91	1.63	3.04	2.48	1.82	3.90
FeO	5.23	4.76	6.37	5.12	–	6.14	4.73	4.11	6.86	8.88	6.30	6.41	6.14	5.79	6.45	8.49
MnO	0.14	0.17	0.13	0.21	0.13	0.22	0.16	0.16	0.15	0.20	0.13	0.12	0.12	0.21	0.14	0.15
MgO	6.58	4.66	6.39	7.86	6.58	9.12	6.50	5.21	9.69	7.47	9.02	7.70	10.33	8.43	7.41	9.15
CaO	8.09	4.60	4.97	6.50	2.87	9.04	8.93	10.02	6.42	5.54	7.45	7.89	2.57	2.12	0.63	2.13
SrO	0.201	0.142	0.189	0.04	0.02	0.08	0.09	0.09	0.08	0.05	0.08	0.06	0.02	0.01	<0.005	0.01
BaO	0.268	0.346	0.246	–	0.106	0.301	0.304	0.327	0.277	0.109	0.206	0.163	0.234	0.174	0.123	0.084
Li_2O	0.012	0.034	0.049	0.042	0.049	0.032	0.021	0.02	0.025	0.02	0.02	0.01	0.027	0.073	0.023	0.033
Na_2O	1.67	1.26	1.74	0.76	0.72	1.27	1.87	2.01	1.58	2.28	1.88	2.37	0.49	0.51	0.07	0.08
K_2O	4.60	5.73	5.59	6.10	5.06	3.88	3.35	3.26	3.38	4.02	4.20	3.36	6.12	6.26	7.46	6.40
P_2O_5	0.54	0.51	0.51	0.85	0.42	0.56	0.49	0.49	0.54	0.65	0.52	0.68	1.00	0.43	0.27	0.68
H_2O^+	1.73	2.92	2.24	3.62	–	2.07	2.40	2.32	–	1.65	1.48	1.23	2.51	3.57	3.26	3.37
H_2O^-	0.21	0.55	0.13	0.14	–	0.18	0.36	0.41	0.11	0.31	0.35	0.18	0.25	0.34	0.68	0.28
CO_2	0.89	2.62	0.16	0.41	0.37	1.20	4.04	5.39	0.98	–	–	–	0.24	0.97	0.05	0.92
F	0.23	0.46	1.56	0.47	1.648	0.61	0.50	0.51	1.452	0.26	0.34	0.13	0.58	2.85	0.74	0.57
C	0.01	0.02	0.03	–	–	<0.01	<0.01	0.05	0.01	–	–	–	<0.01	<0.01	0.04	–
S	0.03	0.23	0.24	<0.01	–	0.02	0.03	0.01	0.01	–	–	–	0.04	0.02	0.03	–
LOI	–	–	–	–	2.71	–	–	–	2.23	2.65	3.09	1.09	–	–	–	–
F-eq.	–0.096	–0.193	–0.656	–0.197	–0.691	–0.256	–0.21	–0.214	–0.611	–0.11	–0.14	–0.05	–0.24	–1.20	–0.31	–0.24
S-eq.	–0.007	–0.057	–0.06	0.00	–	–0.005	–0.007	–0.002	–0.002	–	–	–	–0.01	–0.005	–0.007	–
Sum	98.48	99.53	100.33	99.83	100.21**	99.60	98.63	98.96	98.59**	99.03**	99.56**	99.28**	99.34	99.71	99.3	100.12
FeO_{tot}	6.06	5.85	7.28	7.34	7.77	7.31	6.11	5.35	8.49	10.34	8.02	7.88	8.88	8.02	8.09	12.00
mg#	0.66	0.59	0.61	0.66	0.60	0.69	0.65	0.63	0.67	0.56	0.67	0.64	0.67	0.65	0.62	0.58
K_2O/Na_2O	2.75	4.55	3.21	8.03	7.03	3.06	1.79	1.62	2.14	1.84	2.23	1.42	12.5	12.3	106	80
Laboratory	1	1	1	2	4	1	1	1	1	3	3	3	1	1	1	2

Rocks: Mi = minette, Ke = kersantite, Sp = spessartite, GL = greisenized lamprophyre, Di = altered microdiorite

mg# = Mg/(Mg + Fe) with total Fe, atomic values

* – total Fe as Fe_2O_3

** – sum includes LOI and F, other separately analyzed volatile components are omitted

Laboratories: 1 – Czech Geological Survey, Prague, wet methods; 2 – Charles University in Prague, Faculty of Science, wet methods; 3 – Institute of Geology, Academy of Science of the Czech Republic, Prague, wet methods; 4 – Activation Laboratories, Ltd., Ancaster, XRF (Seifert 2008)

Sample locations: 1 – minette, Horní Krupka, drill hole E-4, sample 21; 2 – minette, Horní Krupka, drill hole E-18A, sample 25; 3 – minette, Horní Krupka, drill hole E-18, sample 29; 4 – minette, Horní Krupka, Vrchoslav adit (dump), sample 626; 5 – minette, Horní Krupka, Vrchoslav adit (dump), Seifert (2008); 6 - kersantite-minette, Horní Krupka, drill hole E-18 A, 38.5-39.7 m; 7 - kersantite, Preisselberg, adit No. 2, measure point 2119; 8 - kersantite, Preisselberg, adit No. 2, cross cut PI2 eastern part; 9 – kersantite associated with a quartz vein, Preisselberg, adit No. 2; 10 – kersantite, Horní Krupka, Večerní Hvězda adit (dump); 11 – kersantite, Preisselberg, adit No. 2 (dump); 12 – spessartite, Horní Krupka, Večerní Hvězda adit (dump); 13 - greisenized lamprophyre, Horní Krupka, drill hole E-4, sample 18; 14 - greisenized lamprophyre, Preisselberg, drill hole P-12, 159 m; 15 - greisenized lamprophyre, Horní Krupka, drill hole E-4, sample 37; 16 – altered microdiorite, Horní Krupka, drill hole E-5, sample 57.

Tab. 2b Chemical composition of mafic dyke rocks from the Krupka ore district (trace elements excluding REE)

	1	2	3	4	5	6	7	8	9	10	11	12	13	14	15	16
Sample	E-4-21	E-18A-25	E-18A-29	Vr-626	Krupka-626	E-18A-8	PrG2-2119	PrG2-PI2	PrG2-19	LA161	LA170	LA162	E-4-18	P-14-159	E-4-37	E-5-57
Rock type	Mi	Mi	Mi	Mi	Mi	Ke	Ke	Ke	Ke	Ke	Ke	Sp	GL	GL	GL	Di
Sc (ppm)	15.1	27.2	26.8	17.4	22	29.3	18	36	13	24.7	22.9	20.6	23.2	31	36.6	22.8
V	141	132	132	–	144	175	153	155	159	166	132	172	149	152	176	173
Cr	350	450	350	348	399	460	471	482	467	504	547	399	580	509	400	760
Co	47	30	27	18	29	50	45	40	42	33	27	30	46	42	36	32
Ni	–	–	–	195	152	–	303	297	315	149	277	129	–	366	–	309
Cu	60	~300	~200	30	12	11	26	29	29	24	28	14	33	32	23	24
Zn	124	159	375	184	67	235	161	140	243	185	201	283	210	276	415	205
Ga	14	24	28	23	24	25	15	28	28	20	20	20	24	40	25	20
As	–	–	–	15.9	34	–	383	385	298	–	–	–	–	69	–	23
Mo	2	3	5	27.7	3	3	3	3	2	–	–	–	3	2	2	1.14
Sn	14	130	230	51.6	48	190	75	112	127	127	53	58	80	62	150	24.3
Li	56	158	227	196	232	148	97	93	116	95	96	52	125	339	107	153
Be	3	7	9	6.6	10	9	7	8	10	9.2	18	5.6	6	19	18	6.3
B	<9	<9	<9	8	–	<9	<9	<9	<9	–	–	–	<9	18	100	47
Rb	150	380	580	303	787	390	263	269	381	591	512	372	450	1431	710	122
Cs	13	26	26	53.5	57.2	34	25	27	38	75	39	44	78	122	90	99
Sr	1700	1200	1600	373	130	700	804	810	629	357	672	426	190	66	<50	24.3
Ba	2400	3100	2200	1880	949	2700	2722	2929	2480	1027	1845	1514	2100	1558	1100	752
Y	29.5	32.0	48.0	24.7	22	21.7	26	31	23	32.9	28.0	31.4	31.2	9	24.9	34
Zr	315	332	321	678	342	518	482	487	392	417	458	443	585	514	388	381
Hf	–	–	–	22.1	12.2	–	5	31	26	11.2	9.6	8.1	–	30	–	8
Nb	10	10	14	24.5	23	39	35	37	32	15.5	29.3	18.1	38	45	20	17.7
Ta	–	–	–	–	1.5	–	1	<1	–	0.93	1.4	0.78	4	<1	–	1.22
W	<5	<5	<5	14.8	9	–	3	4	< 5	–	–	–	–	9	<5	3.2
Bi	<2	2	2.6	8.2	0.7	1	<2	<2	10	–	–	–	9	<2	<2	4.7
Pb	15	15	21	8.3	<5	40	91	91	25	–	30	2.8	12	<7	36	100
Th	26	29.7	26.9	31.2	38	65.7	17	55	41	21.1	45.7	23.6	63.1	53	40.9	17.8
U	<15	20	21	5.9	7.7	20	<15	<15	<15	4.6	8.8	4.7	20	29	<15	6.1
Lab/Method	1	1	1	2, 6	Seifert	1	1	1	1	2–5	2–5	2–5	1	1	1	2–6

Rocks: Mi = minette, Ke = kersantite, Sp = spessartite, GL = greisenized lamprophyre, Di = altered microdiorite

Laboratories and methods: 1 – Czech Geological Survey, Praha, combination of methods (see text for details); 2 – Charles University in Prague, Faculty of Science, AAS (Co, Cr, Cs, Cu, Li, Ni, Pb, Rb, Sr, V, Zn); 3 – Charles University in Prague, Faculty of Science, ICP-MS (Ba, Be, Hf, Sn, Ta); 4 – University of Vienna, Austria, XRF (Ga, Nb, Sc, Y, Zr); 5 – Exploranium CZ, Brno (U, Th); 6 – Analytika, a. s. Praha, ICP-MS (As, B, Ba, Be, Bi, Ga, Hf, Mo, Nb, Sc, Sn, Ta, Th, U, V, W, Y, Zr); Seifert – Activation Laboratories Ltd., Ancaster, Canada, combination of methods (Seifert 2008).

Tab. 2c Chemical composition of mafic dyke rocks from the Krupka ore district (rare earth elements)

	1	2	3	4	5	6	7	8	9	10	11	12	13	14	15	16
Sample	E-4-21	E-18A-25	E-18A-29	Vr-626	Krupka-626	E-18A-8	PrG2-2119	PrG2-PI2	PrG2-19	LA161	LA170	LA162	E-4-18	P-14-159	E-4-37	E-5-57
Rock type	Mi	Mi	Mi	Mi	Mi	Ke	Ke	Ke	Ke	Ke	Ke	Sp	GL	GL	GL	Di
La (ppm)	81.1	90.5	105.4	83.7	62.0	62.7	99.4	102.0	87.8	80.0	88.0	69.0	108.3	69.5	30.3	64.6
Ce	204.1	225.9	241.7	146.0	118.0	142.0	205.3	217.6	168.4	134.0	146.0	118.0	242.1	150.7	76.0	115.4
Pr	26.5	27.6	29.3	14.1	13.1	18.4	22.5	23.5	20.6	19.4	20.3	17.5	28.3	16.1	9.1	12.1
Nd	104.1	111.5	113.7	52.4	45.9	60.8	74.1	81.7	66.0	67.0	65.0	61.0	104.8	51.7	35.7	52.2
Sm	15.44	16.53	17.49	11.7	7.9	8.78	9.34	9.00	8.14	11.9	10.1	10.9	15.35	6.36	5.80	10.47
Eu	4.00	4.32	3.90	3.29	1.92	2.47	2.47	2.64	2.19	3.35	2.37	2.65	2.90	1.82	1.40	2.04
Gd	10.29	11.42	12.93	8.42	6.3	6.57	7.09	7.27	6.44	8.02	6.28	7.33	10.12	4.41	5.63	–
Tb	1.83	1.94	2.35	1.24	0.8	1.10	<1	1.12	<1	1.2	0.92	1.09	2.08	<1	<1	1.11
Dy	6.73	7.04	9.86	5.74	4.2	4.65	4.43	4.38	4.34	6.37	4.76	5.72	6.51	3.10	4.71	–
Ho	0.68	<0.3	<0.3	0.97	0.8	<0.3	0.6	0.7	0.88	1.15	0.86	1.05	<0.3	0.49	<0.3	1.18
Er	2.47	2.66	4.20	2.70	2.2	1.90	1.60	2.16	1.76	3.13	2.32	2.76	2.41	1.71	2.04	–
Tm	<0.3	<0.3	0.56	0.32	0.33	<0.3	<0.3	<0.3	<0.3	0.42	0.29	0.36	<0.3	<0.3	<0.3	1.09
Yb	2.56	2.85	5.18	2.44	1.9	2.24	2.08	2.23	2.16	2.81	2.07	2.39	2.71	1.71	2.47	2.59
Lu	0.32	0.36	0.68	0.41	0.26	0.29	0.33	0.31	0.23	0.42	0.30	0.34	0.34	0.21	0.33	0.47
$(La/Yb)_N$	26.31	26.09	16.09	21.19	24.75	22.44	31.27	34.15	39.62	19.77	30.45	21.06	33.06	34.35	9.53	14.27
Eu/Eu*	0.97	0.96	0.79	1.01	0.83	0.99	0.93	0.99	0.92	1.05	0.91	0.90	0.71	1.05	0.75	0.68
Lab/Method	1	1	1	2	Seifert	1	1	1	1	3	3	3	1	1	1	4

$(La/Yb)_N$ = elemental ratio of La and Yb normalized to average chondrite composition (McDonough and Sun 1995)
Eu/Eu* = europium anomaly calculated using the geometric mean of chondrite-normalized abundances of Sm and Gd or Sm and Tb (sample 16)
Laboratories and methods: 1 – Czech Geological Survey, Praha, ICP; 2 – Analytika, a. s. Praha, ICP-MS; 3 – Charles University in Prague, Faculty of Science, ICP-MS; 4 – Institute of Nuclear Research, Academy of Sciences of the Czech Republic, Řež, INAA; Seifert – Activation Laboratories Ltd., Ancaster, Canada, ICP-MS (Seifert 2008).

(Rock 1991). The Th/U ratios vary strongly from 1.29 to 7.33 and are distinctly decoupled from the chondritic, mantle or crustal ratios (3.92–4.31; McDonough and Sun 1995; Rudnick and Gao 2003).

The chondrite-normalized REE patterns are characterized by an enrichment of LREE over HREE and no or minor negative Eu anomaly (Fig. 11). The $(La/Yb)_N$ values are generally high (kersantites: 22.4–31.3, minettes 16.1–24.8, spessartite 21.1), but in the greisenized lamprophyres vary widely (9.5–34.4). The total abundances of REE as well as the LREE/HREE ratios are identical to those in lamprophyres from the Jáchymov district and elsewhere in the KHE (Štemprok et al. 2008; Seifert 2008) and, indeed, worldwide (Rock 1991; Fig. 11).

The concentrations of LILE are high (Li = 52–372 ppm, Rb = 150–924 (1431) ppm, Cs = 13–122 ppm). The contents of alkali earths are high as well (Ba = 752–3100 ppm, Sr = 24–1700 ppm). It is difficult to distinguish whether the high variability is due to the primary enrichment in lamprophyric magmas or the superimposed effects of greisenization.

The primitive mantle-normalized multielement spidergram shows an overall enrichment in most of the trace elements over their respective concentrations in island-arc and continental-arc basalts (Fig. 12). The lamprophyres are characterized by a high enrichment in Li, Cs, Rb and Th, a moderate enrichment in Ba, and negative Nb ± Ta and Ti anomalies. In contrast to representative world lamprophyres (Rock 1991), they exhibit regional enrichment in Li, Rb, Cs, Th, U and Zr. This pattern is similar to that of Late Variscan lamprophyres of the Black Forest (Hegner et al. 1998), the Sudetes (Awdankiewicz 2007), the KHE (Seifert 2008) and Lusatia (Abdelfadil et al. 2013).

6.2. Element mobility and mass changes during greisenization

The greisenization of lamprophyres leads to substantial modal and chemical changes. The primary mafic minerals (mainly clinopyroxene and phlogopite) with their alteration products (amphibole, chlorite) and feldspars are replaced by an assemblage of lithian phlogopite and topaz with variable amounts of fluorite, apatite and titanium oxides. The related whole-rock compositional changes consist of depletion of Na_2O, CaO, Sr ± Ba, moderate depletion in REE, and addition of LILE (Li, Rb, Cs), F and Sn. The depletion pattern of Na and alkali earths is characteristic of granite-related

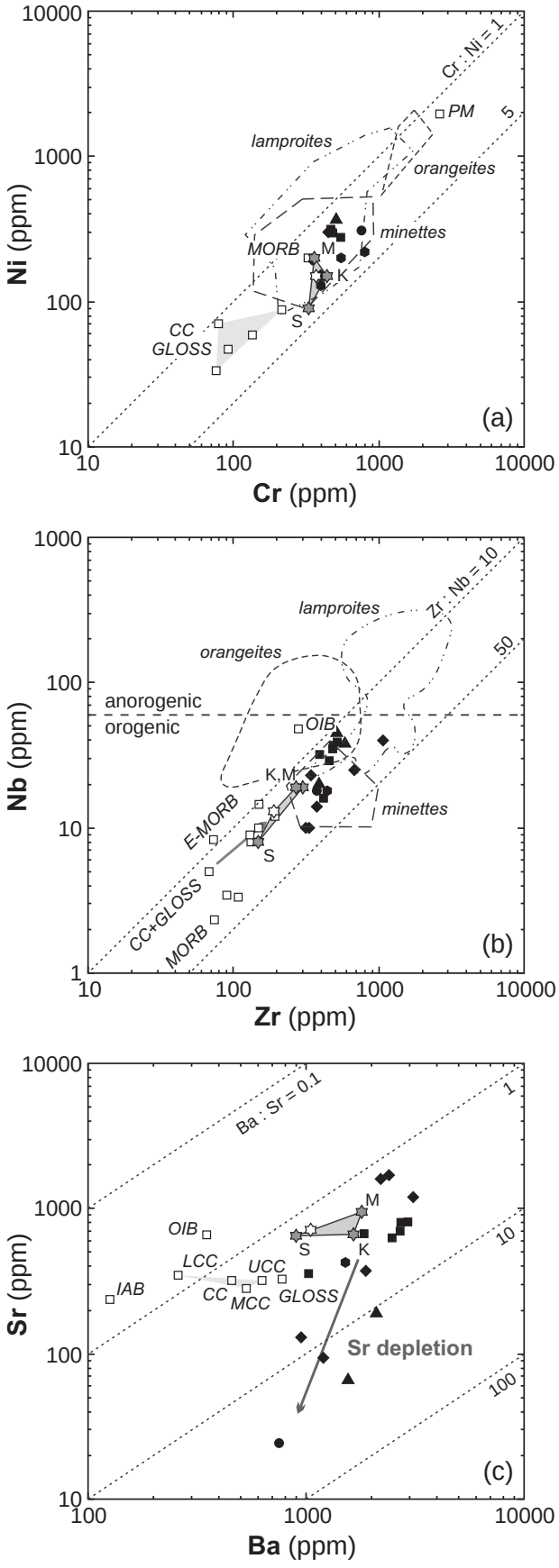

greisen alteration as well (Schwartz and Surjono 1990; Halter et al. 1996). The concentrations of LILE, F and Sn are positively correlated and exceed those reported in average lamprophyres (Fig. 13). The Li, Rb and F are not decoupled during hydrothermal addition and their ratios remain within the range observed in unaltered lamprophyres worldwide: F/Li = 15–130, Rb/Li = 1.3–8.0. By contrast, the enrichment in Sn exceeds that of LILE and F by about one order of magnitude and, as a consequence, the Sn/F and Sn/Li ratios increase up to 0.05 and 1.5, respectively (Fig. 14).

The high field strength elements (HFSE) are nearly conserved and the correlations in Al_2O_3, TiO_2 and Zr suggest that they were probably immobile during greisenization, similarly to other hydrolytic alteration systems (MacLean and Barrett 1993; Halter et al. 1996). The increase in the Al_2O_3 and Zr concentrations by a factor of 1.11–1.21 during the greisenization of kersantites and minettes demonstrates that the alteration was accompanied by an overall mass loss of 10–18 % (Fig. 13), consistent with the substantial formation of porosity, which facilitated the hydrothermal replacement.

7. Discussion

7.1. Spatial distribution of lamprophyre dykes

Lamprophyre dykes are distributed throughout the KHE and Fichtelgebirge/Smrčiny metamorphic complexes, which both host large granite batholiths, and in the adjacent Sub-Erzgebirge Basin (Kramer 1976; Seifert 2008). Granite batholiths associated with lamprophyres were documented in the greisen-type ore provinces of Alaska (Sainsbury et al. 1968; Sainsbury 1969) and Transbaikalia (Troshin 1978; Litvinovskii et al. 1995; Kozlov and Efremov 1999; Abushkevich and Syritso 2005, 2007) and in tin-bearing districts with tourmaline–chlorite-bearing sulphide mineralization in Mesozoic provinces of Yakutia and Chukotka (Korostelev 1977; Indolev

Fig. 10 Trace-element variation diagrams comparing the lamprophyres and other mafic dykes from the Krupka district with the global lamprophyre averages (Rock 1991), main geochemical reservoirs and representative rock series. Symbols are as in Fig. 8. Abbreviations: CC – continental crust (Rudnick and Gao 2003), GLOSS – global oceanic subducting sediment (Plank and Langmuir 1998), IAB – island arc basalt (Kelemen et al. 2003), LCC – lower continental crust (Rudnick and Gao 2003), MCC – middle continental crust (Rudnick and Gao 2003), MORB – mid-ocean ridge basalt (Arevalo and McDonough 2010), OIB – ocean island basalt (Sun and McDonough 1989), PM – primitive mantle (McDonough and Sun 1995), UCC – upper continental crust (Rudnick and Gao 2003). The variation fields of orangeites, lamproites and minettes are from Mitchell and Bergman (1991). The boundary between orogenic and anorogenic potassic rocks is based on Leat et al. (1986).

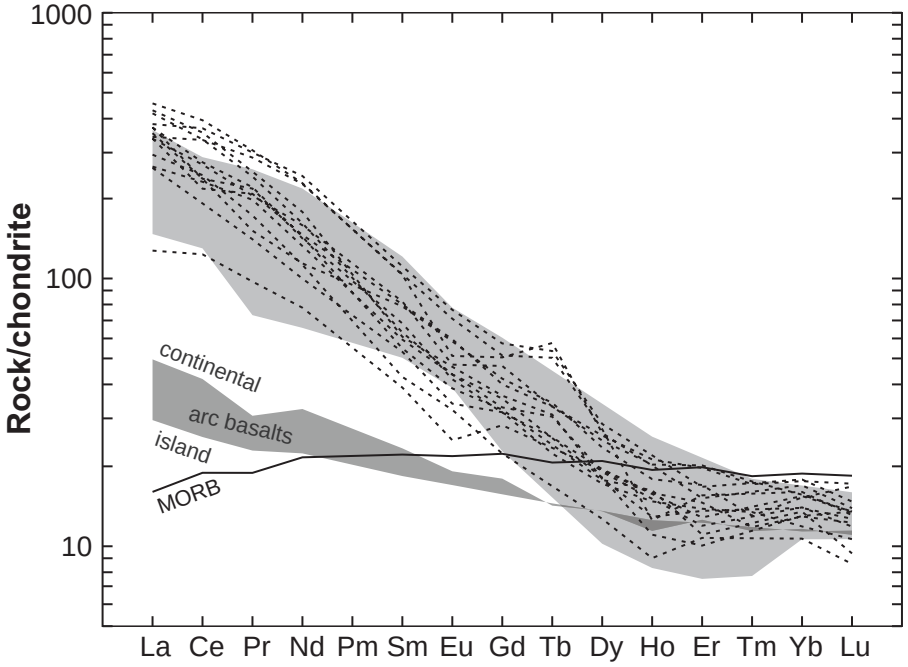

Fig. 11 Chondrite-normalized (McDonough and Sun 1995) REE spidergram of representative lamprophyres and mafic dykes from the Krupka district. The light grey field outlines the variation range of lamprophyres (Rock 1991), the dark grey field corresponds to primitive basalts from the island and continental arc settings (Kelemen et al. 2003). The average mid-ocean ridge basalt is taken from Arevalo and McDonough (2010).

1979; Lugov et al. 1986). In these diverse geological settings, lamprophyres occur jointly with felsic dykes while mafic dykes such as dolerites and microdiorites are subordinate. In the KHE, minettes and kersantites are present in approximately equal proportions, in various tectonic structures but generally independent of the exposures of Late Variscan granites (Watznauer 1964; Holub and Štemprok 1999). Many lamprophyre dykes are spatially related to deep faults (*Tiefstörungen*; Kramer 1976). This relationship was remarkably documented in the Western KHE (Štemprok et al. 2008), but it is less clear in its eastern part. The presence of the deep-seated structures in the Eastern KHE, which could have focused the ascending magmas and hydrothermal fluids, is indicated by (i) the NW–SE strike and alignment of the hidden granite ridges of younger granites, (ii) the NW-trending distribution of tin mineralization (Dalmer 1890; Tischendorf 1963). This crustal structure, which hosts most of the lamprophyre

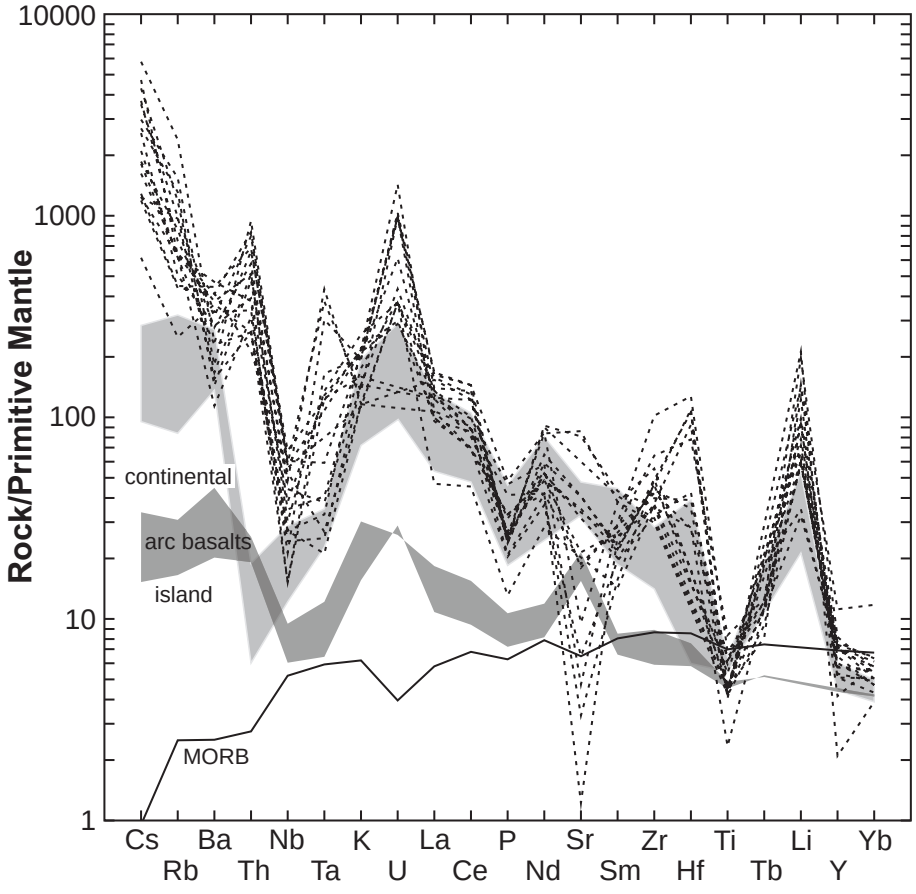

Fig. 12 Primitive Mantle-normalized (McDonough and Sun 1995) spidergram for representative lamprophyres and other mafic dykes from the Krupka district. Data sources are as in Fig. 11. The order of elements follows increasing compatibility in oceanic basalts (Sun and McDonough 1989; Arevalo and McDonough 2010).

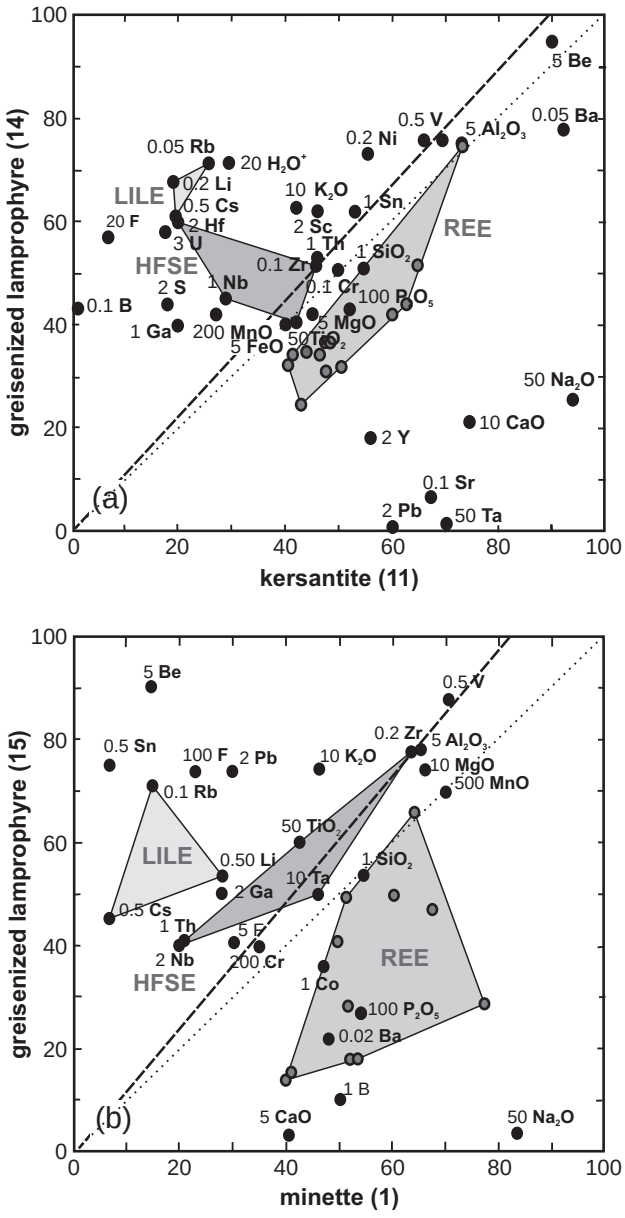

Fig. 13 Isocon diagrams (Grant 1986) illustrating the whole-rock chemical changes during greisenization of kersantite (a) and minette (b). The dotted line is a reference slope of unity (no net mass change) whereas the solid line is the preferred isocon based on the presumed immobile behaviour of Al and Zr.

outcrops in the Eastern KHE, extends from Niederbobritzsch over Schellerhau to Krupka (Kramer 1976). At Krupka, this NW–SE structure additionally hosts the Sn–W greisen mineralization that is spatially associated with the partly hidden granite plutons (Štemprok et al. 1994). These structures control the loci of lamprophyre magma emplacement, intrusion of younger, mostly tin-bearing granites, and infiltration of postmagmatic hydrothermal fluids, which partly shared their ascent paths with the mafic and felsic magmas.

7.2. Age of lamprophyre emplacement and temporal relationships to granites

The kersantites and spessartites in Krupka are correlated by means of whole-rock composition to the LD1 lamprophyre group of the Western and Central KHE (Seifert 2008), which predated the emplacement of the KHE batholith at 330–319 Ma (Tichomirowa and Leonhardt 2010). The minette at Vrchoslav has been assigned to the LD2 lamprophyre group (Seifert 2008), emplaced at 315 Ma and predating the intrusion of the Preisselberg II albite–zinnwaldite granite at Krupka (Štemprok et al 1994; Seifert 2008). The age of greisenization at Zinnwald determined to be between 312.6 ± 2.1 Ma and 314.9 ± 2.3 Ma (Seifert et al. 2011) agrees with assignment of the Krupka minettes to the LD2 lamprophyre group at 315 Ma, but disagrees with the crystallization age of the Teplice rhyolite (308 Ma; Hoffmann et al. 2013) which is often greisenized in the Cínovec/Zinnwald and Krupka districts and its formation predated the greisen alteration.

In the drill hole E-5, the Preisselberg biotite granite is intersected by a microdiorite dyke (depth 375.9–376.5 m), thus providing evidence for an additional stage of emplacement of mafic/lamprophyre dykes postdating the intrusion of the highly evolved granites (Pälchen et al. 1984; Štemprok et al. 1994). This intrusive stage corresponds to the LD3 group of feldspar-phyric lamprophyres (Seifert 2008), independently documented by the presence of altered feldspar phenocrysts. The occurrence of several intrusive stages of lamprophyres is further supported by the emplacement of minettes and kersantites in tectonic structures of variable strikes in the Eastern KHE (Kramer 1976). However, mutual cross-cutting relationships of groups of individual dykes and swarms of kersantites and minettes have not yet been observed in the Krupka district.

7.3. Sources of volatiles and hydrothermal alteration of lamprophyres

The studied lamprophyres are substantially altered, with no relics of olivine and strong replacement of clinopyroxene by secondary amphibole. These features are common to numerous lamprophyre occurrences worldwide and are a hallmark of calc-alkaline lamprophyres in granite provinces (Wimmenauer 1973; Rock 1991). In addition to this alteration, the formation of globular carbonates in pilitic olivines and uralitized clinopyroxenes and of carbonate–quartz veinlets are typical of the Krupka lamprophyres. The carbon in carbonates is isotopically light ($\delta^{13}C_{PDB}$ = –5.0 to –7.7 ‰) indicating an origin during CO_2 flow from Earth's mantle (Žák et al. 2001). The sulphur isotope composition of accessory iron sulphides in spessartite

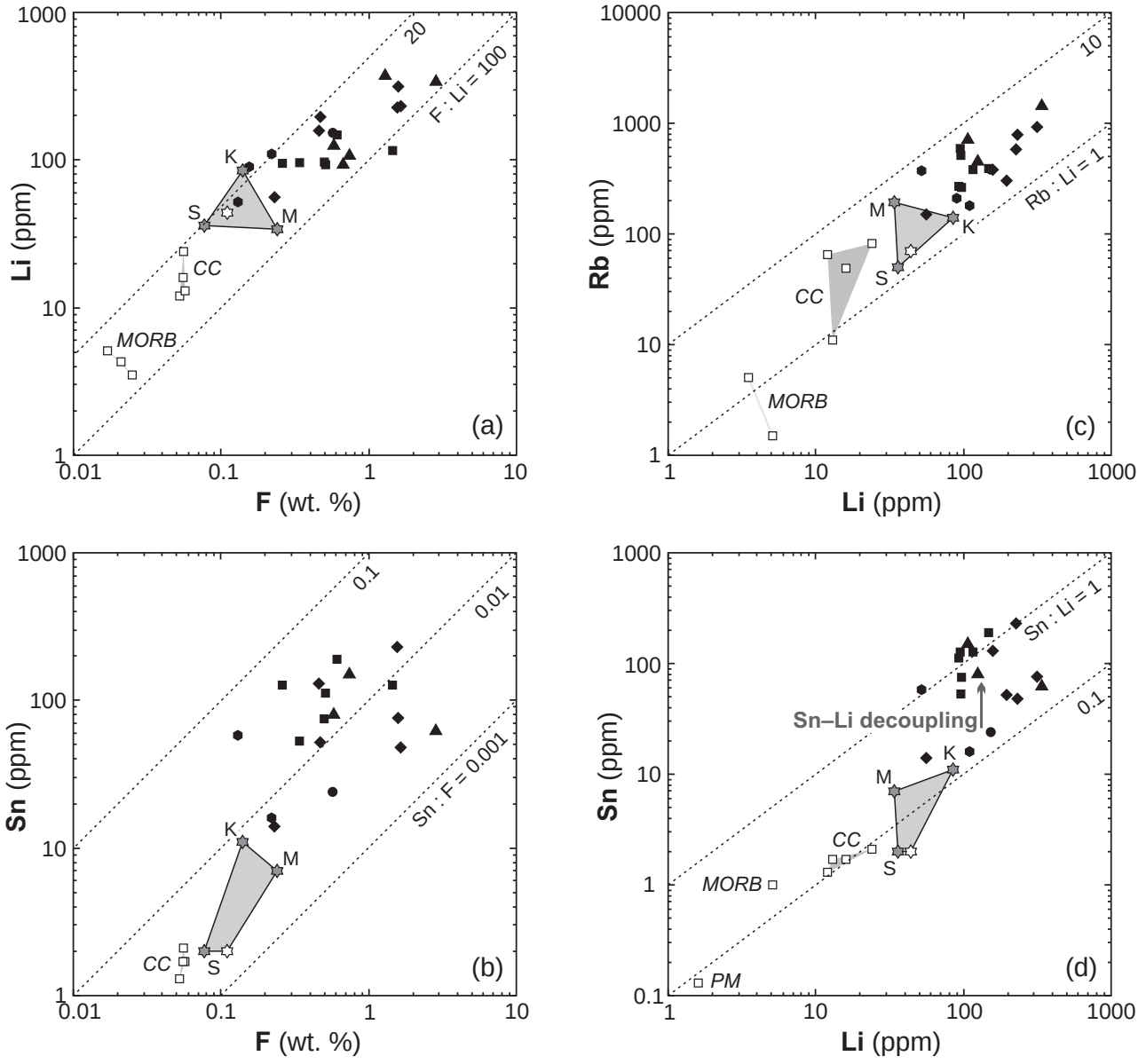

Fig. 14 Variation diagrams illustrating the concentrations of lithophile, volatile and ore elements in lamprophyres and other mafic dykes from the Krupka district and their comparison to global lamprophyre averages (Rock 1991) and other geochemical reservoirs. Symbols are as in Fig. 8. Abbreviations: CC – upper to lower continental crust (Rudnick and Gao 2003), MORB – mid-ocean ridge basalt (Arevalo and McDonough 2010), PM – primitive mantle (McDonough and Sun 1995).

($\delta^{34}S_{CDT}$ = 1.5 ‰) falls within the upper mantle range while that in minette ($\delta^{34}S_{CDT}$ = 6.9 ‰) indicates a crustal source or a fractionation of H_2S. The oxygen isotope composition ($\delta^{18}O_{PDB}$ = 19.0 and 23.0 ‰ in minette and spessartite, respectively) points to a derivation from crustal lithologies or aqueous fluids (Žák et al. 2001; Štemprok et al. 2008).

The greisenization of lamprophyres was younger than the late- and post-magmatic breakdown of olivine and clinopyroxene. During the alteration, the mineral assemblage of lamprophyres was progressively replaced by lithium dark micas, topaz and fluorite. This mineral association differs considerably from that observed in many greisens derived from granites, which is dominated by quartz and white mica (Rundkvist et al. 1971; Štemprok 1987). The lamprophyre dyke crosscutting the gneiss sequence in the P-10 drill hole at Preisselberg hosts elevated amounts of cassiterite (Janečka and Štemprok 1968), which indicates that lamprophyre dykes may represent preferential trap for precipitation of hydrothermal Sn mineralization.

The greisenization of lamprophyres was associated with a significant enrichment in Sn, F and Li and depletion in Na_2O and CaO due to hydrolytic breakdown of

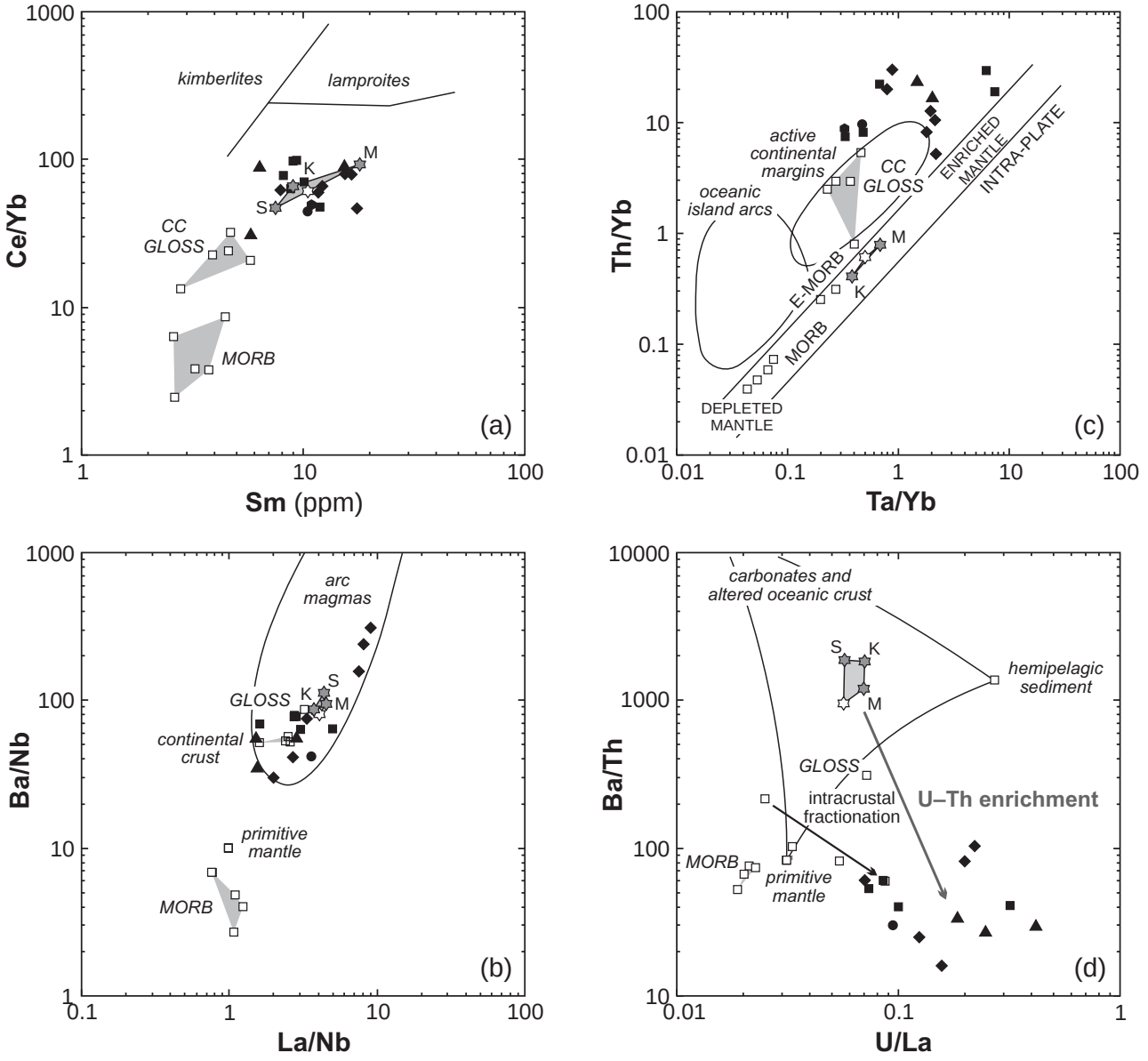

Fig. 15 Petrogenetic trace-element variation diagrams illustrating the relationships between the lamprophyres and other mafic dykes from the Krupka district, global lamprophyre averages (Rock 1991) and the main geochemical reservoirs. Symbols are as in Fig. 8. Abbreviations: CC – upper to lower continental crust (Rudnick and Gao 2003), GLOSS – global oceanic subducting sediment (Plank and Langmuir 1998), MORB – mid-ocean ridge basalt (Arevalo and McDonough 2010), PM – primitive mantle (McDonough and Sun 1995). Fields of representative rock types or products from various geodynamic settings are based on: (a) Rock (1991); (b) Jahn and Zhang (1984); (c) Pearce (1983), Wilson (1989); (d) Patino et al. (2000).

feldspars. The MgO and P_2O_5 abundances did not change substantially due to local redistribution and overall preservation of these two constituents in lithium dark micas and apatite, respectively. The enrichment of lamprophyres in the LILE (e.g., Li and Cs) is a characteristic feature of the Krupka district. By contrast, in the Freiberg area, the Sn mineralization is limited to the occurrences of cassiterite in distal polymetallic veins with unknown parental intrusive body (see Fig. 1), whereas the Krupka ore district hosts the Sn–W mineralization that is closely spatially associated with the lithium-mica alkali-feldspar granites. The lamprophyres in the latter region are typically enriched in Li, Rb, and Cs as a consequence of their location in the proximal geochemical dispersal aureole of the highly evolved granite intrusions.

7.4. Origin of lamprophyric magmas

The calc-alkaline lamprophyres of the KHE are characterized by high Cr and Ni concentrations, low Sr contents, and low V/Cr ratios (Kramer 1976; Seifert 2008), which indicate their origin from a depleted lithospheric

mantle. The low CaO concentrations and elevated Mg/Ca ratios require the derivation from residual harzburgites, and the contents of MgO as well as the Mg/Fe ratios suggest that they represent near-primary mantle melts, whereby the degree of partial melting did not exceed *c.* 20 % (Rock 1991). The strong LREE/HREE enrichment supports a melting in the garnet stability field, i.e. at pressures exceeding ~24 kbar (Gasparik 2003). However, the LREE abundances and the Ce/Yb ratios do not reach the levels observed in lamproites or kimberlites (Fig. 15a). The REE–HFSE variations (e.g, La/Nb, Ta/Yb) are in a broad agreement with those observed for continental crust or subduction/arc component (Fig. 15b–c). Similarly, the high concentrations of Rb, Ba, Pb, Sr, U and Th, high Th/La and low Sm/La ratios in the Late Variscan European lamprophyres (Turpin et al. 1988; Awdankiewicz 2007; Seifert 2008; Abdelfadil et al. 2013) were attributed to the contribution from the continental crust (Turpin et al. 1988; Awdankiewicz 2007; Romer and Hahne 2010) or to the infiltration of aqueous fluids/hydrous melts from subducted altered oceanic crust and its terrigenous or pelagic sediments (Prouteau et al. 2001; Owen 2008).

The LILE (Ba), HFSE (U, Th) and REE (La) signatures of lamprophyres correspond to comparable contributions from the primitive mantle and subducted pelagic sediments (e.g., Owen 2008). The distinct signature of lamprophyres from the Eastern KHE reflects an additional strong and selective enrichment in U and Th (Fig. 15d). This feature is consistent with the involvement of oxidized saline fluids *en route* from the subducting slab to the mantle wedge, which are capable of transporting significant quantities of U and Th (Bali et al. 2011). In this scenario, the variably focused fluid flow produces geochemical heterogeneities in the upper mantle (Zack and John 2007), which may be responsible for a spatial coexistence of spessartites, kersantites and minettes in the Krupka, Freiberg and Bärenstein ore districts. In detail, the high Rb/Sr and low Ba/Sr ratios may indicate the predominance of phlogopite over amphibole in the mantle source (Guo et al. 2004). The involvement of variably metasomatized mantle sources in the lamprophyre origin (Turpin et al. 1988; Seifert 1997) can also serve as indicator of the metal endowment during the post-Variscan hydrothermal ore-forming processes in the KHE (e.g., Baumann et al. 2000).

8. Concluding remarks

Lamprophyres in the Eastern KHE are spatially associated with Variscan tin-bearing granites. Both lithologies were affected by greisenization, which is documented by the formation of topaz-bearing mica-rich greisens and glimmerites with local cassiterite accumulation at the expense of lamprophyres. Furthermore, lamprophyre dykes are intersected by Sn–W-bearing greisen veins and mineralized quartz veins. Both fresh and altered lamprophyres have substantially elevated concentrations of LILE when compared with average calc-alkaline lamprophyres worldwide, and the lamprophyre-derived greisens are in addition enriched in Li, Sn, F, Rb and Cs and depleted in Na, Ca and Ba. The spatial link between lamprophyres and greisens suggests accessibility of the upper crust to mantle products – melts and/or fluids – at the time of formation of Sn mineralization in the Eastern KHE.

The association of lamprophyres and greisens in the Krupka district, however, does not imply any genetic relationship between the emplacement of lamprophyric magma into the upper crust and the hydrothermal fluids that formed the Sn–W mineralization. The spatial link was most likely structurally controlled and the lamprophyres LD1 and LD2 (some preceding the granite emplacement) were followed by a single greisenization event superimposed on lamprophyres, their host rocks as well as granites (Štemprok et al. 1994).

The intrusion of kersantite and spessartite dykes predated the emplacement of the KHE granites, which implies that the mantle metasomatism occurred before the generation of granitic magmas in the continental crust. The lamprophyre magmas, considered to be volatile-rich and geochemically specialized melts, would be plausible sources of volatiles and other elements contributing to the melting of the lower crust. This anatexis would produce melts parental to the ore-bearing granites, as already suggested for lamprophyric and rhyolitic intrusions and associated tin and polymetallic mineralization in the KHE (Seifert 2008). The enrichment in F of the metasomatized upper mantle is well documented by the presence of fluorides or F-rich amphibole and biotite in peridotite xenoliths (Klemme 2004; Aiuppa et al. 2009). Similarly, many lamprophyres have shoshonitic nature and the spatially associated rare-metal granites worldwide are frequently K-rich as well (Beskin et al. 1979). The metasomatism by interaction of mantle-derived mafic and crustal granitic melts has been postulated for Sn-mineralized granites during Mesozoic magmatic activity at the Chukotka Peninsula (Kozlov and Efremov 1999). The potassium enrichment, exceeding 5 wt. % K_2O globally in the Eastern Pluton, the Teplice rhyolite and the Altenberg–Frauenstein microgranites (Štemprok et al. 2003), is greater than most representative granite averages (e.g., Vinogradov 1962; Condie 1981). Mantle volatiles, including halogens, could have served as a possible ligand for the ore element transport and as a fluxing agent which substantially contributed to prolonged generation of granitic partial melts in the lower crust in the districts

with rare metal mineralization. It appears plausible that the lamprophyric magmas could have contributed their constituents to felsic melts in the lower crust as suggested by Štemprok and Seifert (2011) and affected their differentiation to rare-metal enriched melts.

*Acknowledgements***.** This study was supported by the Grant Agency of the Charles University Nr. 165/1998 (to M. Š.), the Grant Agency of the Czech Republic through Grant No. 205/09/0630 (to F. V. H.), the Czech Science Foundation Nr. P210/12/0986 (to D. D.), the Ministry of Education, Youth and Sports of the Czech Republic through Research Plan No. MSM0021620855 and the Charles University Research Support Project P44. We would like to thank Marta Chlupáčová, Edvín Pivec, Miloš Lang and Jiří K. Novák for their assistance during various stages of this study. We thank Richard Scrivener for providing us with unpublished data on the Cornwall lamprophyres. We appreciate the critical reviews by Marek Awdankiewicz and Thomas Seifert as well as careful editorial handling by Vladislav Rapprich and Vojtěch Janoušek, which all helped to improve the manuscript.

References

Abdelfadil KM, Romer RL, Seifert T, Lobst R (2013) Calc-alkaline lamprophyres from Lusatia (Germany). Evidence for a repeatedly enriched mantle source. Chem Geol 353: 230–245

Abushkevich VS, Syritso LF (2005) Composition and chemistry of dyke rocks in rare-metal Khangilai ore knot in Eastern Transbaikalia. Apatity 1: 7–9 (in Russian)

Abushkevich VS, Syritso LF (2007) Isotopic-Geochemical Model of the Li–F Granite Formation in the Khangilai Ore Knot in Eastern Transbaikalia. Nauka, St. Petersburg, pp 1–147 (in Russian)

Aiuppa A, Baker DR, Webster JD (2009) Halogens in volcanic systems. Chem Geol 263: 1–18

Arculus RJ (2003) Use and abuse of the terms calcalkaline and calcalkalic. J Petrol 44: 929–935

Arevalo R jr, McDonough WF (2010) Chemical variations and regional diversity observed in MORB. Chem Geol 271: 70–85

Ashley PM, Cook NDJ, Hill RL, Kent JR (1994) Shoshonitic lamprophyre dykes and their relation to mesothermal Au–Sb veins at Hillgrove, New South Wales, Australia. Lithos 32: 249–272

Awdankiewicz M (2007) Late Palaeozoic lamprophyres and associated mafic subvolcanic rocks of the Sudetes (SW Poland): petrology, geochemistry and petrogenesis. Geol Sudetica 39: 11–117

Bali E, Audétat A, Keppler H (2011) The mobility of U and Th in subduction zone fluids: an indicator of oxygen fugacity and fluid salinity. Contrib Mineral Petrol 161: 591–613

Baumann L, Kuschka E, Seifert T (2000) Lagerstätten des Erzgebirges. Enke, Stuttgart, pp 1–300

Beck R (1914) Die Zinnlagerstätten von Graupen in Böhmen. Jb Geol Reichsanst 64: 269–306

Beskin SM, Larin VN, Marin YuB (1979) Rare-Metal Granite Formations. Nedra, Leningrad, pp 1–280 (in Russian)

Bianchini G, Wilson M (1999) Tertiary–Quaternary magmatism within the Mediterranean and surrounding regions. In Durand B, Jolivet L, Horvath F, Seranne M (eds) The Mediterranean Basins: Tertiary extension within the Alpine Orogen. Geological Society of London Special Publications 156: 141–168

Bonin B (1990) From orogenic to anorogenic settings: evolution of granitoid suites after a major orogenesis. Geol J 25: 261–270

Boynton WV (1984) Cosmochemistry of the rare earth elements: meteorite studies. In: Henderson P (ed) Rare Earth Element Geochemistry. Elsevier, Amsterdam, pp 63–114

Breiter K (2012) Nearly contemporaneous evolution of the A- and S-type fractionated granites in the Krušné hory/Erzgebirge Mts., Central Europe. Lithos 151: 105–121

Chrt J, Malásek F (1984) Hidden upper surface of the Krušné hory granites between Cínovec and Krupka. Geol Průzk 26: 305–309 (in Czech)

Condie KC (1981) Archean Greenstone Belts. Elsevier, Amsterdam, pp 1–434

Dalmer K (1890) Erläuterungen zur geologischen Specialkarte des Königsreiches Sachsen, Section Altenberg–Zinnwald. Commision bei W. Engelmann, Leipzig, pp 1–110

Eisenreich M, Breiter K (1993) Krupka deposit of Sn–W–Mo ores in the eastern Krušné hory Mts. Věst Ústř Úst Geol 68: 15–22

Fiala F (1959) The Teplice quartz porphyry between Krupka, Cínovec, Dubí and Mikulov, and the associated rocks. Sbor Ústř Úst Geol, Geol 26: 445–478 (in Czech)

Finger F, Roberts MB, Haunschmid B, Schermaier A, Steyrer HB (1997) Variscan granitoids of central Europe: their typology, potential sources and tectonothermal relations. Mineral Petrol 61: 67–96

Foley SF, Venturelli G, Green DH, Toscani L (1987) The ultrapotassic rocks: characteristics, classification and constrains for petrological models. Earth Sci Rev 24: 81–143

Förster H-J, Romer RL (2010) Carboniferous magmatism. In: Linnemann U (ed) Pre-Mesozoic Geology of Saxo-Thuringia: From the Cadomian Active Margin to the Variscan Orogen. Schweizerbart, Stuttgart, pp 287–308

Förster H-J, Tischendorf G, Trumbull RB, Gottesmann B (1999) Late collisional granites in the Variscan Erzgebirge (Germany). J Petrol 40: 1613–1645

Fortey NJ (1992) The Exeter volcanic rocks: geochemistry. British Geological Survey Technical Report, Mineralogy and Petrology Series WG/92/7, pp 1–45

Frost BR, Frost CD (2008) A geochemical classification for feldspathic igneous rocks. J Petrol 49: 1955–1969

Gäbert C, Beck R (1903) Erläuterungen zur geologischen Specialkarte des Königsreichs Sachsen, Blatt 120. Commision bei W. Engelman, Leipzig, pp 1–107

Gasparik T (2003) Phase Diagrams for Geoscientists. An Atlas of the Earth's Interior. Springer, Berlin, pp 1–462

Gerstenberger H (1989) Autometasomatic Rb enrichment in highly evolved granites causing lowered Rb–Sr isochron intercepts. Earth Planet Sci Lett 93: 65–75

Grant JA (1986) The isocon diagram – a simple solution to Gresen's equation for metasomatic alteration. Econ Geol 81: 1976–1982

Guo F, Fan W, Wang Y, Zhang M (2004) Origin of early Cretaceous calc-alkaline lamprophyres from the Sulu orogen in eastern China: implications for enrichment processes beneath continental collisional belts. Lithos 78: 291–305

Halter W, Williams-Jones AE, Kontak DJ (1996) The role of greisenization in cassiterite precipitation at the East Kemptville tin deposit, Nova Scotia. Econ Geol 91: 368–395

Hegner E, Kölbl-Ebert M, Loeschke J (1998) Postcollisional Variscan lamprophyres (Black Forest, Germany), $^{40}Ar/^{39}Ar$ phlogopite dating, Nd, Pb, Sr isotope and trace element characteristics. Lithos 45: 395–411

Hoffmann U, Breitkreuz C, Breiter K, Sergeev S, Stanek K, Tichomirowa M (2013) Carboniferous–Permian volcanic evolution in Central Europe – U/Pb ages of volcanic rocks in Saxony (Germany) and northern Bohemia (Czech Republic). Int J Earth Sci 102: 73–99

Holub FV (2003) Ultrapotassic quartz melasyenite from Nebahovy near Prachatice, South Bohemia – geochemically anomalous lamproite rocks. Zpr geol Výzk v Roce 2002: 164–166 (in Czech)

Holub FV, Štemprok M (1999) Variscan lamprophyres and granitoid-related mineralizations: Comparison of the Krušné hory–Erzgebirge and Central Bohemian batholiths. In: Stanley C (ed) Mineral Processes: Processes to Processing. A. A. Balkema, Rotterdam, pp 365–368

Hoth K, Wasternack J, Berger H-J, Breiter K, Mlčoch B, Schovánek P (1994) Geologische Karte Erzgebirge/Vogtland 1:100 000. Sächsisches Landesamt für Umwelt und Geologie, Dresden

Hösel GA (1972) Position, Aufbau sowie tektonische Strukturen des Erzgebirges. Geologie 21: 436–456

Indolev LN (1979) Dikes in the Ore Districts of Eastern Yakutia. Nauka, Moscow, pp 1–193 (in Russian)

Irvine TN, Baragar WR (1971) A guide to the chemical classification of the common igneous rocks. Can J Earth Sci 8: 523–548

Jahn BM, Zhang ZQ (1984) Archean granulite gneisses from eastern Hebei province, China: rare earth geochemistry and tectonic implication. Contrib Mineral Petrol 85: 224–243

Janečka J, Štemprok M (1967) New ore geology and petrographic data from the western part of the Krupka district. Věst Ústř Úst Geol 42: 133–136 (in Czech)

Janoušek V, Holub FV (2007) The causal link between HP–HT metamorphism and ultrapotassic magmatism in collisional orogens: case study from the Moldanubian Zone of the Bohemian Massif. Proc Geol Assoc 118: 75–86

Kelemen PB, Hanghøj K, Greene AR (2003) One view of the geochemistry of subduction-related magmatic arcs, with an emphasis on primitive andesite and lower crust. In: Rudnick RL (ed) The Crust. Treatise of Geochemistry 3: Elsevier, Amsterdam, pp 593–659

Kempe U, Bombach K, Matukov D, Schlothauer T, Hutschenreuther J, Wolf D, Sergeev S (2004) Pb/Pb and U/Pb zircon dating of subvolcanic rhyolite as a time marker for Hercynian granite magmatism and Sn mineralization in the Eibenstock granite, Erzgebirge, Germany: considering effects of zircon alteration. Miner Depos 39: 523–535

Klemme S (2004) Evidence for fluorite melts in the Earth's mantle formed by liquid immiscibility. Geology 32: 441–444

Korostelev VI (1977) Dike complex of the Upper-Khandygskii granitoid massif of granodiorites. In: Korostelev VI, Dmitriev SD, Kolodeznikov II, Savvinov NM, Tomtozov IA, Tschurbaev FI (eds) Geology and the Distribution Pattern of Resources in Yakutia. Yakutsk State University Publishing House, Yakutsk, pp 52–60 (in Russian)

Kozlov VD, Efremov SV (1999) Potassic alkali basaltoids and geochemical specialization of the associated rare-metal granites. Russ Geol Geoph 40: 973–985

Kramer W (1976) Genese der Lamprophyre im Bereich der Fichtelgebirgisch-Erzgebirgischen Antiklinalzone. Chem Erde 35: 1–49

Kramer W (1988) Magmengenetische Aspekte der Lithosphärenentwicklung. Series in Geological Sciences, Akademie Verlag, Berlin, pp 1–136

Kramer W, Seifert W (1994) Mica-lamprophyres and related volcanics of the Erzgebirge and metallogenic aspects. In: Seltmann R, Kämpf H, Möller P (eds) Metallogeny of Collisional Orogens. Czech Geological Survey, Prague, pp 159–165

Krmíček L (2010) Pre-Mesozoic lamprophyres and associated dyke intrusions of the Bohemian Massif (Czech Republic, Poland, Germany, Austria): a review. Acta Mus Moraviae, Sci Geol 95: 3–61 (in Czech)

Krmíček L, Cempírek J, Havlín A, Přichystal A, Houzar S, Krmíčková M, Gadaš P (2011) Mineralogy and petrogenesis of a Ba–Ti–Zr-rich peralkaline dyke from Šebkovice (Czech Republic): recognition of the most lamproitic Variscan intrusion. Lithos 121: 74–86

Leake BE, Woolley AR, Arps CES, Birch WD, Gilbert MC, Grice JD, Hawthorne FC, Kato A, Kisch HJ, Krivovichev VG, Linthout K, Laird J, Mandarino JA, Maresch WV, Nickel EH, Rock NMS, Schumacher JC, Smith DC, Stephenson NCN, Ungaretti L, Whittaker EJW, Youzhi G (1997) Nomenclature of amphiboles. Can Mineral 35: 219–246

Leat PT, Jackson SE, Thorpe RS, Stillman CJ (1986) Geochemistry of bimodal basalt–subalkaline/peralkaline rhyolite provinces within the southern British Caledonides. J Geol Soc London 143: 259–276

Le Maitre RW (ed, 2002) Igneous Rocks. A Classification and Glossary of Terms. Cambridge Univ Press, Cambridge, pp 1–236

Linnemann U (ed) (2008) Das Saxothuringikum. Abriss der präkambrischen und paläozoischen Geologie von Sachsen und Thüringen. Geol Saxon 36: 1–163

Litvinovskii BA, Antipin VS, Reyf FG, Kuzmin MI (1995) Rare metal and palyngenetic granitoids of Transbaikalia and related mineralization. Excursion Guide. Transbaikalia Field Meeting, August 1–15, 1995. Irkutsk–Ulan Ude–Moscow, pp 1–99

Lobach-Zhuchenko SB, Chekulaev VP, Ivanikov VV, Kovalenko AV, Bogomolov ES (2000) Late Archean high-Mg and subalkaline granitoids and lamprophyres as indicators of gold mineralization in Karelia (Baltic Shield). In: Krementsky A, Lehmann B, Seltmann R (eds) Ore-bearing Granites of Russia and Adjacent Countries. IMGRE, Moscow, Intas 93-1783 Project, IGCP 373 Project, pp 193–211

Lugov SF, Kryuchov AS, Makeev BV (1986, eds) Geology of Tin Deposits of the USSR (3 volumes). Nedra, Moscow, pp 1–332, 1–429, 1–200 (in Russian)

Luhr JF, Carmichael ISE, Varekamp JC (1984) The 1982 eruptions of El Chichon volcano, Choapas, Mexico: mineralogy and petrology of the anhydrite-bearing pumices. J Volcanol Geotherm Res 23: 69–108

MacLean WH, Barrett JL (1993) Lithogeochemical techniques using immobile elements. J Geochem Explor 48: 109–133

McDonough WF, Sun SS (1995) The composition of the Earth. Chem Geol 120: 223–253

McNeil AM, Kerrich R (1986) Archean lamprophyre dikes and gold mineralization, Ontario. The conjunction of LILE-enriched magmas, deep crustal structures and gold concentrations. Can J Earth Sci 23: 324–343

Mingram B, Kröner A, Hegner E, Krentz O (2004) Zircon ages, geochemistry and Nd isotopic systematics of pre-Variscan orthogneisses from the Erzgebirge, Saxony (Germany), and geodynamic interpretation. Int J Earth Sci 93: 706–727

Mitchell RH, Bergman SC (1991) Petrology of Lamproites. Plenum Press, New York, pp 1–447

Mlčoch B, Skácelová Z (2010) Geometry of the Altenberg–Teplice caldera revealed by the borehole and seismic data in its Czech part. J Geosci 55: 217–229

Müller D, Groves DI (1993) Direct and indirect associations between potassic igneous rocks, shoshonites and gold–copper deposits. Ore Geol Rev 8: 383–406

Müller D, Rock NMS, Groves DI (1992) Geochemical discrimination between shoshonitic and potassic volcanic rocks from different tectonic settings: a pilot study. Mineral Petrol 46: 259–289

Müller A, Seltmann R (2002) Plagioclase mantled K-feldspar in Carboniferous porphyritic microgranite of Altenberg and Frauenstein, Eastern Erzgebirge/Krušné hory. Bull Geol Soc Finland 74: 53–79

Mizera J, Řanda Z (2010) Instrumental neutron and proton activation analyses of selected geochemical reference materials. J Radiol Nucl Chem 284: 157–163

Novák JK (1994) Mineral associations at the Krupka (Graupen) greisenized stock. In: Seltmann R, Kämpf H, Möller P (eds) Metallogeny of the Collisional Orogens. Czech Geological Survey, Prague, pp 61–69

Novák JK, Pivec E, Holub FV, Štemprok M (2001) Greisenization of lamprophyres in the Krupka Sn–W district in the eastern Krušné hory/Erzgebirge, Czech Republic. In: Piestrzyński A (ed) Mineral Deposits at the Beginning of the 21st Century. Sweets and Zeilinger Publishers, Lisse, pp 465–488

Owen JP (2008) Geochemistry of lamprophyres from the Western Alps, Italy: implications for the origin of an enriched isotopic component in the Italian mantle. Contrib Mineral Petrol 155: 341–362

Pälchen W, Wetzel HU, Lobin M, Seltmann R (1984) Spätvariszicher Magmatismus und Bruchtektonik im Osterzgebirge. 31. Jahrestagung Gesellschaft für geologische Wissenschaften, Berlin, pp 53–60

Patino LC, Carr MJ, Feigenson MD (2000) Local and regional variations in Central American arc lavas controlled by variations in subducted sedimentary input. Contrib Mineral Petrol 138: 265–283

Pearce JA (1983) The role of sub-continental lithosphere in magma genesis at destructive plate margins. In: Hawkesworth CJ, Norry MJ (eds) Continental Basalts and Mantle Xenoliths. Shiva, Nantwich, pp 230–249

Pietzsch K (1962) Geologie von Sachsen. Deutscher Verlag der Wissenschaften, Berlin, pp 1–870

Pivec E, Holub FV, Lang M, Novák JK, Štemprok M (2002) Rock-forming minerals of lamprophyres and associated mafic dykes from the Krušné hory/Erzgebirge (Czech Republic). J Czech Geol Soc 47: 23–32

Plank T, Langmuir CH (1998) The chemical composition of subducting sediment and its consequences for the crust and mantle. Chem Geol 145: 325–394

Prelević D, Foley SF, Cvetković V, Romer RL (2004) Origin of minette by mixing of lamproite and da-

cite magmas in Veliki Majdan, Serbia. J Petrol 45: 759–792

Prouteau G, Scaillet B, Pichavant M, Maury R (2001) Evidence for mantle metasomatism by hydrous silicic melts derived from subducted oceanic crust. Nature 410: 197–200

Rock NMS (1991) Lamprophyres. Van Nostrand Reinhold, Glasgow, pp 1–286

Rock NMS, Groves DI, Perring CS, Golding SD (1989) Gold, lamprophyres, and porphyries: what does their association mean? Econ Geol 84: 609–625

Romer RL, Hahne K (2010) Life of the Rheic ocean: scrolling through the shale record. Gondwana Res 17: 236–253

Romer RL, Thomas R, Stein HJ, Rhede D (2007) Dating multiply overprinted Sn-mineralized granites – examples from the Erzgebirge, Germany. Miner Depos 42: 337–359

Romer RL, Förster H-J, Štemprok M (2010) Age of late-Variscan magmatism in the Altenberg–Teplice Caldera (Eastern Erzgebirge/Krušné hory). Neu Jb Mineral, Abh 187: 289–305

Rudnick RL, Gao S (2003) Composition of the continental crust. In Rudnick RL (ed) The Crust. Treatise of Geochemistry 3: Elsevier, Amsterdam, pp 1–64

Rundkvist DV, Denisenko VK, Pavlova IG (1971) Greisen Deposits. Nedra, Moscow, pp 1–327 (in Russian)

Sainsbury CL (1969) Geology and ore deposits of the Central York Mountains, Western Seward Peninsula, Alaska. US Geol Surv Bull 1287: pp 1–101

Sainsbury CL, Hamilton JC, Huffman C Jr (1968) Geochemical cycle of selected trace elements in the tin–tungsten–beryllium district. US Geol Surv Bull 1242F, pp 1–42

Schumacher JC (1997) Appendix 2. The estimation of the proportion of ferric iron in the electron-microprobe analysis of amphiboles. Canad Mineral 35: 238–246

Schwartz MO, Surjono (1990) Greisenization and albitization at the Tikus tin–tungsten deposit, Belitung, Indonesia. Econ Geol 85: 691–713

Seifert T (1994) Zur Metallogenie des Lagerstättendistriktes Marienberg (Ostteil des Mittelerzgebirgischen Antiklinalbereiches). Doctoral dissertation, TU Bergakademie Freiberg, pp 1–174

Seifert T (1997) Mantle metasomatism and associated late Variscan Sn and base metal mineralization in the Erzgebirge (Germany). In Hatton CJ (ed) International Symposium on Plumes, Plates & Mineralization, Abstracts. University of Pretoria, pp 89–90

Seifert T (2008) Metallogeny and Petrogenesis of Lamprophyres in the Mid-European Variscides. IOS Press Millpress, Amsterdam, pp 1–303

Seifert W, Kramer W (2003) Accessory titanite: an important carrier of zirconium in lamprophyres. Lithos 71: 81–98

Seifert T, Atanasova P, Gutzmer J, Pfänder J (2011) Mineralogy, geochemistry and age of greisen mineralization in the Li–Rb–Cs–Sn–W deposit Zinnwald, Erzgebirge, Germany. Mineral Mag 75: 18–33

Sejkora J, Breiter K (1999) The historical ore district of Krupka, Krušné hory Mts, Czech Republic. Bull mineral-petrol Odd Nár Muz (Praha) 7: 29–45 (in Czech)

Semiz B, Çoban H, Roden MF, Özpinar Y, Flower MFJ, McGregor H (2012) Mineral composition in cognate inclusions in Late Miocene–Early Pliocene potassic lamprophyres with affinities to lamproites from the Denizli region, Western Anatolia, Turkey: implications for uppermost mantle processes in a back-arc setting. Lithos 134–135: 253–272

Strnad L, Mihaljevič M, Šebek O (2005) Laser ablation and solution ICP-MS determination of REE in USGS BIR-1G, BHVO-2G and BCR-2G glass reference materials. Geost Geoanal Res 29: 303–314

Sylvester PJ (1998) Post-collisional strongly peraluminous granites. Lithos 45: 29–44

Sun SS, McDonough WF (1989) Chemical and isotopic systematics of oceanic basalts: implications for mantle composition and processes. In: Saunders AD, Norry MJ (eds) Magmatism in the Ocean Basins. Geological Society of London Special Publications 42: 313–345

Štemprok M (1987) Greisenization (a review). Geol Rundsch 76: 169–175

Štemprok M, Seifert T (2011) An overview of the association between lamprophyric intrusions and rare metal mineralization. Mineralogia 42: 121–162

Štemprok M, Novák JK, David J (1994) The association of the granites and tin–tungsten mineralization in the eastern Krušné hory (Erzgebirge), Czech Republic. Monograph Series on Mineral Deposits 31, Gebrüder Bornträger, Berlin–Stuttgart, pp 97–129

Štemprok M, Holub FV, Dolejš D, Pivec E, Novák JK, Lang M, Chlupáčová M (2001) Petrogenetic Position of Lamprophyres of the Krušné hory Batholith and Their Relationship to Metallogenesis. Unpublished report, Charles University Grant Agency 165/1998, Prague, pp 1–55

Štemprok M, Holub FV, Novák JK (2003) Multiple magmatic pulses of the Eastern Volcano-Plutonic Complex, Krušné hory/Erzgebirge batholith and their phosphorus contents. Bull Geosci 78: 277–296

Štemprok M, Seifert T, Holub FV , Chlupáčová M, Dolejš D, Novák JK, Pivec E, Lang M (2008) Petrology and geochemistry of Variscan dykes from the Jáchymov (Joachimsthal) ore district, Czech Republic. J Geosci 53: 65–104

Tajčmanová L, Connolly JAD, Cesare B (2009) A thermodynamic model for titanium and ferric iron solution in biotite. J Metamorph Geol 27: 153–165

Tichomirowa M, Leonhardt D (2010) New age determinations (Pb/Pb zircon evaporation, Rb/Sr) on the granites from Aue-Schwarzenberg and Eibenstock, Western Erzgebirge, Germany. Z geol Wiss 38: 99–123

Tindle AG, Webb PC (1990) Estimation of lithium contents in trioctahedral micas using microprobe data; application to micas from granitic rocks. Eur J Mineral 2: 595–610

Tischendorf G (1963) Stand der Kenntnisse bei der Suche nach Zinnlagerstätten im Osterzgebirge. Z angew Geol 10: 225–238

Tischendorf G (1986) Variscan ensialic magmatism and metallogenesis in the Ore Mountains – Modelling of the process. Chem Erde 45: 75–104

Tischendorf G (1988). Leucocratic and melanocratic crust-derived magmatism and metallogenesis. The example Erzgebirge. Z geol Wiss 16: 199–223

Tischendorf G, Gottesmann B, Förster HJ, Trumbull RB (1997) On Li-bearing micas: estimating Li from electron microprobe analyses and an improved diagram for graphical representation. Mineral Mag 61: 809–834

Tischendorf G, Rieder M, Förster HJ, Gottesmann B, Guidotti CV (2004) A new graphical presentation and subdivision of potassium micas. Mineral Mag 68: 649–667

Troshin YP (1978) Geochemistry of volatile components in magmatic rocks, haloes and ores of Eastern Transbaikalia. Nauka, Novosibirsk, pp 1–172 (in Russian)

Turpin L, Velde D, Pinte G (1988) Geochemical comparison between minettes and kersantites from the western European Hercynian orogen: trace element and Pb–Sr–Nd isotope constraints on their origin. Earth Planet Sci Lett 87: 73–86

Vinogradov AP (1962) The average contents of chemical elements in the main types of magmatic rocks of the Earth crust. Geokhimiya 1962/7: 555–571 (in Russian)

von Seckendorff V, Timmerman MJ, Kramer W, Wrobel P (2004) New $^{40}Ar/^{39}Ar$ ages and geochemistry of Late Carboniferous–early Permian lamprophyres and related volcanic rocks in the Saxothuringian Zone of the Variscan Orogen (Germany). In: Wilson M, Neumann ER, Timmermann GR, Heremans M, Larsen BT (eds) Permo–Carboniferous Magmatism and Rifting in Europe. Geological Society of London Special Publications 223: 335–359

Wasternack J, Tischendorf G, Hösel G, Kuschka E, Breiter K, Chrt J, Komínek J, Štemprok M (1995) Mineral Resources Erzgebirge–Vogtland/Krušné hory, Map 2, Metals, Fluorite/Barite – Occurrences and Environmental Impact. Sächsisches Landesamt für Umwelt und Geologie, Bereich Boden und Geologie, Freiberg; Czech Geological Survey, Prague

Watznauer A (1964) Der heutige Stand des Lamprophyrsproblems. Geologie 12: 812–820

Weiss D (1983) Methods of Chemical Analysis of Mineral Resources, Volume 2–3. Czech Geological Survey, Prague, pp 157–302

White RW, Powell R, Holland TJB (2007) Progress relating to calculation of partial melting equilibria for metapelites. J Metamorph Geol 25: 511–527

Wilson M (1989) Igneous Petrogenesis. A Global Tectonic Approach. Chapman & Hall, London, pp 1–466

Wimmenauer W (1973) Granites and lamprophyres. Bull Soc Geol France 15: 195–198

Woolley AR, Bergman SC, Edgar AD, Le Bas MJ, Mitchell RH, Rock NMS, Scott Smith BH (1996). Classification of lamprophyres, lamproites, kimberlites and the kalsilitic, melilitic and leucitic rocks. Canad Mineral 34: 175–186

Wyman DA, Kerrich R (1988) Lamprophyres as source of gold. Nature 332: 209–210

Zack T, John T (2007) An evaluation of reactive fluid flow and trace element mobility in subducting slabs. Chem Geol 239: 199–216

Žák K, Štemprok M, Holub FV, Jačková I, Novák JK, Veselovský F (2001) Isotopic composition of sulphur in sulphides and of carbon and oxygen in carbonates from the mafic dykes in the Czech part of the Krušné hory/Erzgebirge. Zpr Geol Výzk v Roce 2000: 111–114 (in Czech)

Žák L (1966) Origin of the molybdenite and feldspar deposit of Krupka. II. Paragenetic relations. Acta Univ Carol, Geol 1966: 167–195